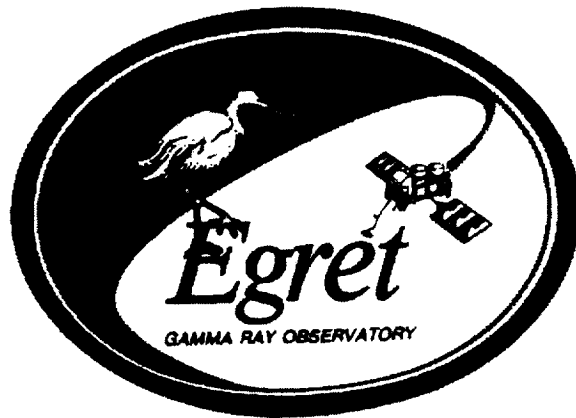


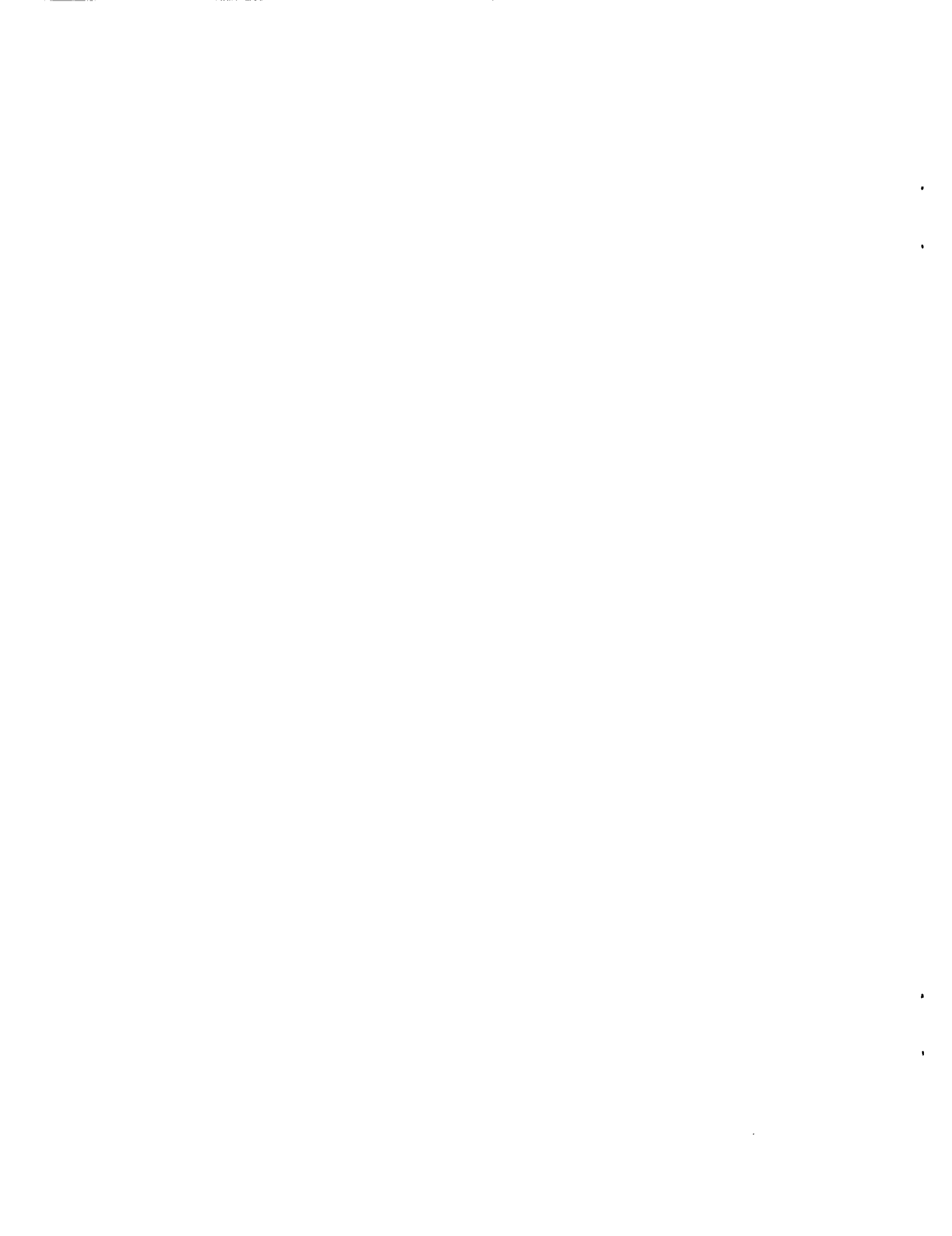
**EGRET Team Papers to be Published in the Proceedings of the  
Fifth Compton Symposium  
Portsmouth, NH  
September 15-17, 1999**

**A. Chen, S. Ritz, Y. C. Lin, P. Sreekumar, D. L. Bertsch, R. Mukherjee, O. Reimer,  
D. J. Thompson, P. M. Wallace et al.**



**Laboratory for High Energy  
Astrophysics**

**NASA Goddard Space Flight Center  
Greenbelt, MD 20771**



**EGRET Team Papers to be Published in the  
Proceedings of the Fifth Compton Symposium  
Portsmouth, NH  
September 15-17, 1999**

Detecting the Attenuation of Blazar Gamma-Ray Emission by Extragalactic Background Light with GLAST .....	A. Chen, S. Ritz
Some Aspects of the Radio Emission of EGRET-Detected Blazars .....	Y.C. Lin et al.
GeV Outbursts in Mrk 501 .....	P. Sreekumar et al.
Spectral Modeling of the EGRET 3EG Gamma Ray Sources Near the Galactic Plane .....	D.L. Bertsch et al.
X-ray and Gamma-ray Observations of the COS-B Field 2CG 075+00 .....	R. Mukherjee et al.
Multiwavelength Studies of the Peculiar Gamma-Ray Source 3EG J1835+5918 .....	O. Reimer et al.
EGRET/COMPTEL Observations of an Unusual, Steep-Spectrum Gamma-Ray Source .....	D.J. Thompson et al.
Preliminary Results from a New Analysis Method for EGRET Data .....	D.J. Thompson et al.
A Systematic Search for Short-term Variability of EGRET Sources .....	P.M. Wallace et al.



# Detecting The Attenuation Of Blazar Gamma-ray Emission By Extragalactic Background Light With GLAST

Andrew Chen, Steven Ritz

*NASA/Goddard Space Flight Center  
Code 661, Greenbelt, MD 20771*

**Abstract.** Gamma rays with energy above 10 GeV interact with optical-UV photons resulting in pair production. Therefore, a large sample of high redshift sources of these gamma rays can be used to probe the extragalactic background starlight (EBL) by examining the redshift dependence of the attenuation of the flux above 10 GeV. GLAST, the next generation high-energy gamma-ray telescope, will for the first time have the unique capability to detect thousands of gamma-ray blazars up to redshifts of at least  $z = 4$ , with enough angular resolution to allow identification of a large fraction of their optical counterparts. By combining recent determinations of the gamma-ray blazar luminosity function, recent calculations of the high energy gamma-ray opacity due to EBL absorption, and the expected GLAST instrument performance to produce simulated samples of blazars that GLAST would detect, including their redshifts and fluxes, we demonstrate that these blazars have the potential to be a highly effective probe of the EBL.

## LUMINOSITY FUNCTION OF GAMMA-RAY BLAZARS

The Energetic Gamma Ray Experiment Telescope (EGRET) has detected more than 60 blazar-type quasars (Mukherjee et al. 1997) emitting gamma rays with  $E > 100$  MeV. These sources are flat-spectrum radio-loud quasars (FSRQs) and BL Lac objects, often exhibiting non-thermal continuum spectra, violent optical variability, and/or high optical polarization. They are also highly variable gamma-ray sources. The EGRET blazars whose optical redshifts have been measured range from  $z = 0.03$  to 2.28. The redshift distribution is consistent with the distribution of FSRQs, which extends up to  $z = 3.8$ .

Chiang & Mukherjee (1998) modeled the evolution and luminosity function of the parent gamma-ray blazar distribution, taking careful account of selection biases, without assuming a correlation between luminosities at gamma-ray and other wavelengths. Parameterizing the luminosity function by

$$\frac{dN}{dVdL_0} = \rho(z)N_0L_0^{-\gamma} \text{ and } L_0 = L/(1+z)^\beta \quad (1)$$

with a maximum cutoff redshift of  $z_{\max} = 5$ , they found  $\rho(z)$  consistent with a constant (no density evolution) and  $\beta = 2.7$  provided the best fit. However, they found that a simple power law in  $L$  failed to model the dearth of blazars below  $z = 1$  adequately.

The best fit was a simple power law with  $\gamma = 2.2$  at high luminosities and a luminosity cutoff of  $L_B = 1.1 \times 10^{46}$  erg s<sup>-1</sup>.

## EXTRAGALACTIC BACKGROUND LIGHT

Gamma-rays traveling through intergalactic space will interact through pair production with the extragalactic background starlight (EBL) emitted by galaxies. The cross section depends on the energies of the target and incident photons. Gamma rays with energy  $E > 10$  GeV are significantly attenuated. Thus, the apparent spectra of gamma-ray emitting objects will be modified at those energies, increasing with increasing redshift. Salamon & Stecker (1998) calculated the opacity out to  $z = 3$ . To estimate the stellar emissivity and spectral energy distributions vs. redshift they adapted the analysis of Fall, Charlot, & Pei (1996), consistent with the Canada-France Redshift Survey. They included corrections for metallicity evolution. They found that the stellar emissivity peaks between  $z = 1$  and 2, leading to a significant redshift-dependent absorption.

## GLAST

The Gamma-ray Large Area Space Telescope (GLAST) is under development with a planned launch in 2005. It is intended to be the successor to EGRET, with a much larger effective area, especially at higher energies ( $\geq 8000$  cm<sup>2</sup> at  $> 1$  GeV), larger field of view and better angular resolution than EGRET. GLAST should be able to reach a flux limit of  $4 \times 10^{-9}$  photons cm<sup>-2</sup> s<sup>-1</sup> after one year, resulting in the detection of thousands of blazars. The improved angular resolution should, in theory, allow a high percentage of optical identifications and possible redshift measurements, depending on the available ground-based resources. The improved high-energy performance should yield accurate flux determinations above 10 GeV for many of these sources.

## PROCEDURE

Using the de-evolved luminosity function proportional to  $L^{-2.2}$  with a minimum cutoff at  $10^{46}$  erg s<sup>-1</sup> according to Chiang & Mukherjee, we generated  $10^6$  blazars. We assigned each one a random redshift  $z$  between 0 and 5 distributed according to the following relations:

$$\begin{aligned} \frac{dN}{dz} &= \frac{dN}{dV} \frac{dV}{dz}, \quad \frac{dN}{dV} = \text{constant}, \\ \frac{dV}{dz} &= \frac{4\pi c}{H_0} \frac{d_l^2(z)(1+z)}{\sqrt{1+2q_0z}}, \\ d_l &= \frac{c}{H_0 q_0} \left[ 1 - q_0 + q_0 z + (q_0 - 1)(2q_0 z + 1)^{1/2} \right], \end{aligned} \quad (2)$$

where  $q_0 = 0.5$  and  $H_0 = 75 \text{ km s}^{-1} \text{ Mpc}^{-1}$ . The flux of each blazar was then calculated according to

$$F = L_0 \frac{(1+z)^{1-\alpha+\beta}}{4\pi d_l^2(z)}, \quad (3)$$

where  $\beta = 2.2$  and  $\alpha = 2.15$ , the average spectral index of the EGRET blazars. This yielded  $\sim 5000$  blazars with observed flux greater than  $4 \times 10^{-9} \text{ photons cm}^{-2} \text{ s}^{-1}$  above  $E > 100 \text{ MeV}$ .

We calculated the  $E > 10 \text{ GeV}$  flux of each by adding two effects. First, each blazar got a random, normally distributed spectral index,  $-2.15 \pm 0.04$ . An index of  $-2.15$  yields a ratio of  $\sim 0.07$  between the two fluxes. We also included the redshift-dependent absorption above  $10 \text{ GeV}$ . The form of the dependence was parameterized from the graph in Salamon and Stecker with metallicity corrections. We set the absorption for  $z > 3$  equal to the absorption at  $z = 3$ , both because it is a conservative assumption and because it is physically realistic (little stellar emissivity for  $z > 3$ ). To produce observed fluxes from these intrinsic fluxes, we assigned each blazar a random position on the sky and added isotropic and Galactic backgrounds appropriate to each flux. The isotropic backgrounds were set to  $4 \times 10^{-6} \text{ photons cm}^{-2} \text{ s}^{-1}$  for  $E > 100 \text{ MeV}$  with a power law index of  $-2.15$ , under the assumption that GLAST may resolve as much as two thirds of the EGRET isotropic background. The Galactic backgrounds were derived from the diffuse model used in EGRET analysis (Hunter et al. 1997).

The fluxes of each blazar at  $E > 1 \text{ GeV}$  and  $10 \text{ GeV}$  were used to generate observed fluxes using the appropriate Poisson distributions. We removed from the sample any blazar within  $10^\circ$  of the Galactic plane and any blazar whose observed flux was less than  $3 \sigma$  above the background flux at  $E > 1 \text{ GeV}$ . We calculated the ratio between these fluxes and the error in that ratio.

We tested the hypothesis that each blazar had the same ratio between the intrinsic fluxes in each energy range (which would result in different measured ratios because of the backgrounds). Figure 1 shows the mean ratio in each redshift bin vs. the ratio predicted by the model of Salamon & Stecker. For comparison, the dashed lines show the same results with the intrinsic spectral variation left intact, but with no extragalactic absorption. Figure 2 shows the same results as Figure 1 when the intergalactic absorption is removed from the observed blazar fluxes.

We repeated the analysis with the mean blazar spectral index changed from  $-2.15$  to  $-2.7$ . Although more blazars have no detected flux above  $10 \text{ GeV}$ , the effects of absorption are still apparent.

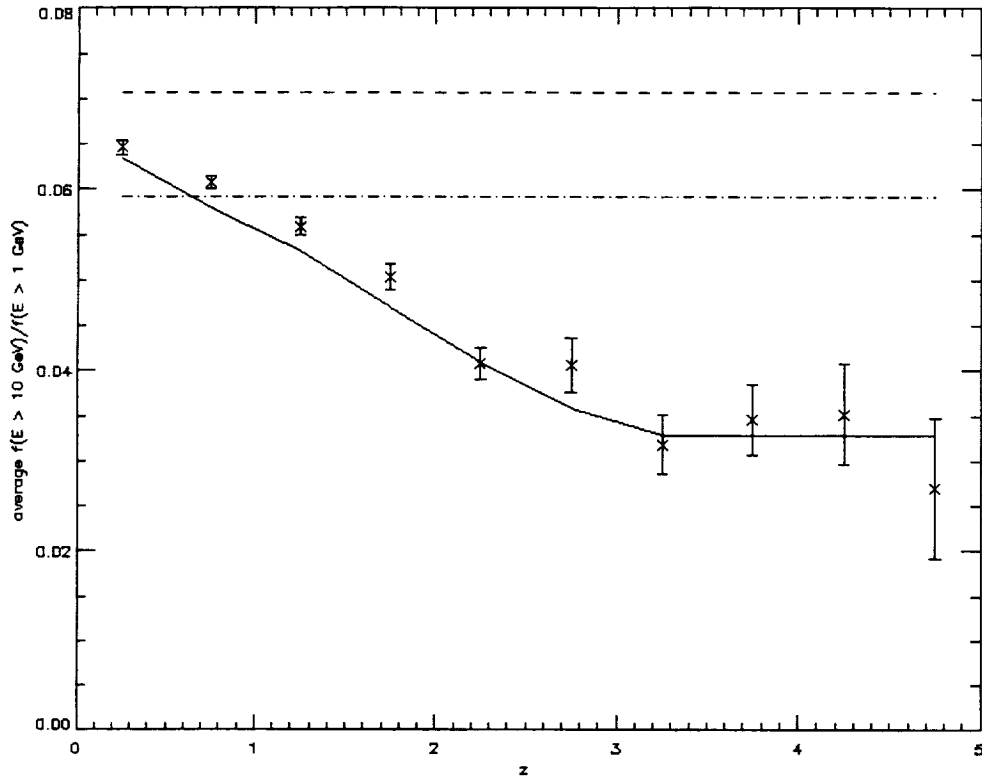


FIGURE 1. Mean flux ratio vs. redshift with extragalactic attenuation.

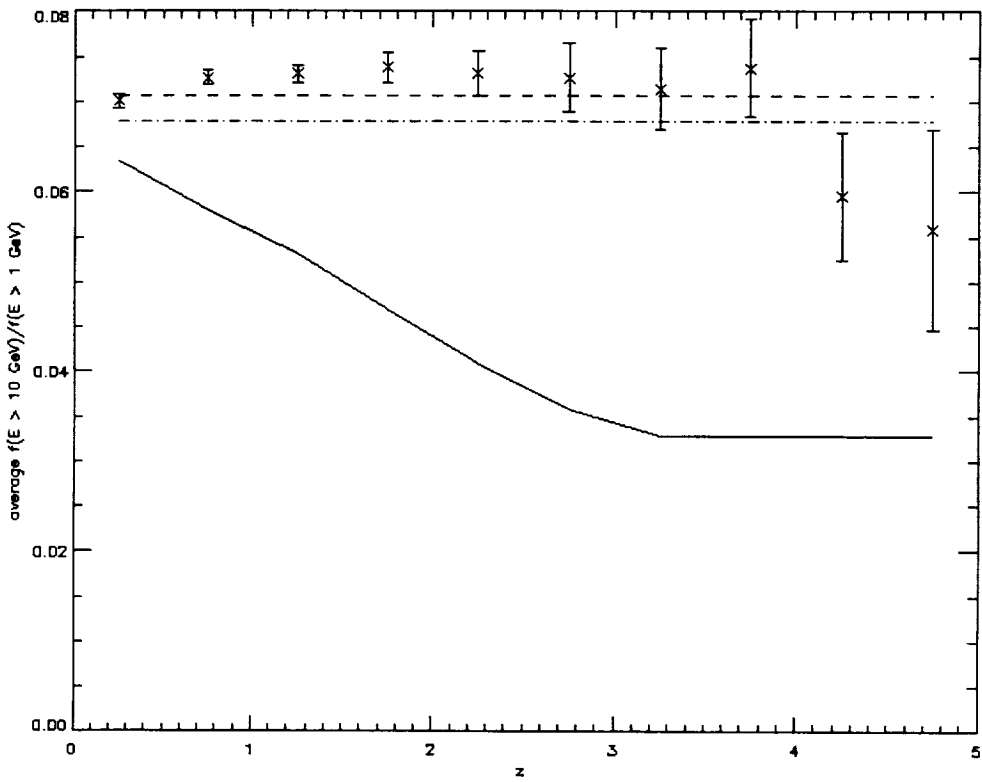


FIGURE 2. Mean flux ratio vs. redshift with no extragalactic attenuation.

## DISCUSSION

Extragalactic attenuation of gamma-rays by low-energy background photons produces a distortion in the spectra of gamma-ray blazars that increases with increasing redshift. Because we cannot distinguish the difference between extragalactic attenuation, internal attenuation, or an intrinsic rolloff in individual blazar spectra, statistical analysis of a large sample of blazars is useful to study EBL absorption. GLAST will be the first instrument capable of observing this large sample at these energies. Our results indicate that the redshift dependence of the attenuation should be easily detectable by GLAST even when the diffuse background is taken into account and possible high energy intrinsic rolloffs are considered.

Selection effects, both from GLAST itself and from optical coverage of redshift determinations, will primarily affect sources with low flux. These sources will have poorly measured flux ratios, and will suffer from optical selection effects due to their more poorly determined positions. Other biases include the location of telescopes, source clustering, and other effects. It will be important to catalog these effects explicitly; in particular, insuring adequate optical coverage may require active preparation and participation. Also, we are repeating this analysis with other EBL models and other blazar luminosity functions that are consistent with EGRET data.

Finally, even after observation of a redshift-dependent effect, the possibility would remain that the spectral evolution of gamma-ray blazars happened to mimic redshift-dependent EBL absorption. Note that blazars are variable, and there are some indications that blazar spectra can become harder when they flare. Evolution in flaring probability could produce the same effect as actual spectral evolution from a statistical standpoint if, for example, a higher percentage of high-redshift blazars were observed in a quiescent phase; however, one would expect the GLAST flux limit to produce a selection effect in the opposite direction. In any case, observation of a redshift-dependent spectral softening will provide an important constraint. Theorists will have to decide the likelihood of an evolutionary conspiracy.

## ACKNOWLEDGEMENTS

We acknowledge useful conversations with Bill Atwood, who first suggested using the large statistics of GLAST AGNs to look for systematic effects of extragalactic background light attenuation with redshift.

## REFERENCES

1. Bloom, E. D., *Space Sci. Rev.* 75, 109 (1996).
2. Chiang, J., and Mukherjee, R., *ApJ* 496, 752 (1998).
3. Chiang, J., et al., *ApJ* 452, 156 (1995).
4. Hunter, S. D., et al., *ApJ* 481, 205 (1997).
5. Mighell, K. J., *ApJ* 518, 380 (1999).
6. Mukherjee, R., et al., *ApJ* 490, 116 (1997).
7. Salamon, M. H., and Stecker, F. W., *ApJ* 493, 547 (1998).



# Some Aspects of the Radio Emission of EGRET-Detected Blazars

Y.C.Lin<sup>1</sup>, D.L.Bertsch<sup>2</sup>, S.D.Bloom<sup>3</sup>, J.A.Esposito<sup>2</sup>, R.C.Hartman<sup>2</sup>,  
S.D.Hunter<sup>2</sup>, D.A.Kniffen<sup>3</sup>, G.Kanbach<sup>4</sup>, H.A.Mayer-Hasselwander<sup>4</sup>,  
P.F.Michelson<sup>1</sup>, R.Mukherjee<sup>5</sup>, A.Mücke<sup>6</sup>, P.L.Nolan<sup>1</sup>, M.K.Pohl<sup>7</sup>,  
O.L.Reimer<sup>4</sup>, and D.J.Thompson<sup>2</sup>

<sup>1</sup> *W. W. Hansen Exp. Phys. Lab., Stanford University, Stanford, CA 94305 USA*

<sup>2</sup> *Code 661, Goddard Space Flight Center, Greenbelt, MD 20771 USA*

<sup>3</sup> *Dept. of Phys. and Astronomy, Hampden-Sydney College, Hampden-Sydney, VA 23943 USA*

<sup>4</sup> *Max-Planck-Institut für Extraterrestrische Physik, Giessenbachstr, D-85748 Garching Germany*

<sup>5</sup> *Barnard College and Columbia University, New York, NY 10027 USA*

<sup>6</sup> *Dept. of Phys. and Mathematical Phys., Univ. of Adelaide, Adelaide, SA 5005 Australia*

<sup>7</sup> *Institut für Theoretische Physik 4, Ruhr-Universität Bochum, 44780 Bochum Germany*

**Abstract.** It has long been recognized that the high-latitude EGRET sources can be identified with blazars of significant radio emission. Many aspects of the relation between high-energy gamma-ray emission and radio emission of EGRET-detected blazars remain uncertain. In this paper, we use the results of the recently published Third EGRET Source Catalog to examine in more detail to what extent the EGRET flux and the radio flux are correlated. In particular we examine the correlation (or the lack of it) in flux level, spectral shape, temporal variation, and detection limit. Many significant previous studies in these areas are also evaluated.

## INTRODUCTION

Ever since EGRET began in 1991 to detect extragalactic objects generally referred to as blazars, the radio emission of such EGRET sources has been found to be closely related to the detected gamma radiation [1–3]. Over the years, many studies have been carried out to investigate the question of radio- $\gamma$ -ray connection. In this paper, we examine and summarize such results for blazars.

## FLUX CORRELATION

Among the EGRET-detected blazars, there are cases when strong  $\gamma$ -ray sources are found to have strong radio fluxes as well, as pointed out by, e.g., Mattox et al.

[4]. But the true nature of the flux correlation between radio and  $\gamma$ -ray emission is more complicated than a simple one-to-one correspondence.

## One-to-One Flux Correlation

Mücke et al. [5] have made a thorough and comprehensive study and found no statistically significant one-to-one correlation between radio flux and EGRET flux. This study provides in-depth analyses on this correlation question. It produces a negative result. Unless future data can sustain a claim otherwise, it is advisable that the radio flux and the EGRET flux should not be regarded as being proportional to each other or having a one-to-one relationship.

## A Possible Correlation Pattern

The radio flux and the high-energy  $\gamma$ -ray flux of EGRET-detected blazars could be correlated in some other ways. In Figure 1, we plot the radio fluxes at 5 GHz versus the EGRET fluxes for  $E > 100$  MeV in individual viewing periods with the EGRET measurement significance  $\sqrt{TS} > 3.0$ . The radio fluxes are taken from the NED database, one value for each source. The EGRET fluxes are those listed in the Third EGRET Catalog [3]. The radio fluxes and the EGRET fluxes are

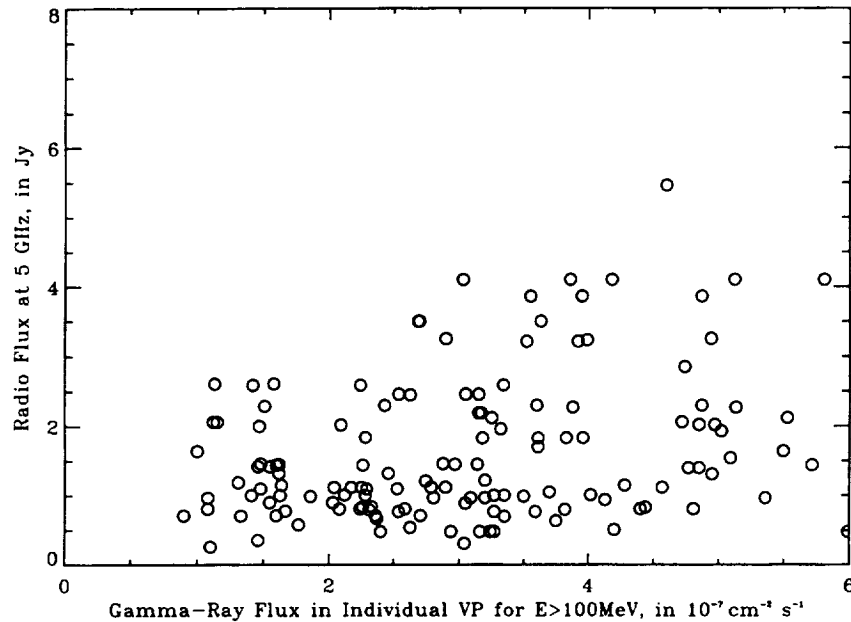


**FIGURE 1.** Radio flux density at 5 GHz vs EGRET flux for  $E > 100$  MeV in individual viewing periods with  $\sqrt{TS} > 3.0$ .

not simultaneous data. One can see that the data points in Figure 1 occupy the lower right half of the graph. The EGRET flux limit at  $\sim 1.0 \times 10^{-7} \text{ cm}^{-2} \text{ s}^{-1}$  for  $E > 100 \text{ MeV}$  reflects the EGRET sensitivity. Beyond the radio flux of  $\sim 2 \text{ Jy}$ , the minimum detected EGRET flux for a source seems to increase with the corresponding radio flux, or at least the EGRET flux level seems more likely to become higher when the radio flux increases in Figure 1. But five of the EGRET-detected blazars, off scale in radio fluxes in Figure 1, do not follow this pattern: 3C 273, 3C 279, 3C 454.3, PKS 0521–365, and PKS 1830–210. These are all very strong radio sources. Their EGRET fluxes are much lower than what this pattern would indicate. At this time, we do not know whether such prominent sources form a true subclass of EGRET-detected blazars or this pattern will disappear under more extensive observations. Furthermore, the variability of radio fluxes, which can easily rearrange the data points in Figure 1, is not considered here. Maybe future high-energy  $\gamma$ -ray missions like the GLAST telescope [6] can confirm or disprove this pattern.

## Flux Correlation during Radio Flares

Valtaoja et al. [7] have published a result on the correlation of EGRET flux with radio flux during radio flares. They have found that during a flare the EGRET flux is correlated with the *increase* in the radio flux at the time of the EGRET measurement, but not to the size of the flare. This study is based on about thirty simultaneous measurements between EGRET observations and Metsähovi 22 GHz monitoring data. The statistical significance is thus not very high, but this is a very interesting result. It is directly related to the radio state at the time of EGRET detection. See the section “RADIO STATE FOR  $\Gamma$ -RAY EMISSION.”

## SPECTRUM CORRELATION

Both the radio spectral indices and the high-energy  $\gamma$ -ray spectral indices of the EGRET-detected blazars extend over large ranges of values. It would be interesting to see if the spectral indices in these two wavebands are correlated in some way. We have calculated the two-point radio spectral indices with data taken from the NED database between 2.7 and 5 GHz, 5 and 31 GHz, and 5 and 90 GHz, for EGRET-detected blazars. The two radio measurements for each spectral index calculation are required to be in the same radio catalog and simultaneous data are used whenever available. The EGRET spectral indices are taken from the Third EGRET Catalog [3]. No correlation whatsoever can be seen between the radio spectral indices and the EGRET spectral indices. It may seem that, although the radio and high-energy  $\gamma$ -ray bands are closely related to each other, the beam of particles that produces one band is unlikely to be the same one that produces the other band. These two bands of radiation are likely to be related to each other at a deeper level of the radiation mechanism.

## RADIO AND EGRET FLUX LIMITS

When the EGRET Team first tried to search for counterparts in radio sources for the high-latitude EGRET sources, the radio flux was restricted to  $>\sim 1$  Jy, later changed to  $>\sim 0.5$  Jy, at 5 GHz in order to reduce the number of source candidates [1]. This has created an uncertainty as to whether the unidentified high-latitude EGRET sources are actually radio sources with fluxes lower than this artificial search limit. To answer this question, Sreekumar et al. [8], Nolan et al. [9], Dingus et al. [10], and Lin et al. [11] have devoted special attention to search for counterparts for the unidentified high-latitude ( $|b| > 10^\circ$ ) EGRET sources in the Second EGRET Catalog [2] among radio sources with fluxes as low as 0.3 Jy at 5 GHz or even lower. Only one possible identification was found in this way. It now appears certain that the radio flux limit of  $\sim 0.5$  Jy at 5 GHz is an intrinsic property of the EGRET-detected blazars for the EGRET detection limit of  $\sim 1.0 \times 10^{-7} \text{ cm}^{-2} \text{ s}^{-1}$  for  $E > 100$  MeV in one viewing period. It is true that some of the EGRET-detected blazars do have radio fluxes below 0.5 Jy at 5 GHz [3]. Furthermore, some of the radio sources with fluxes above 0.5 Jy at 5 GHz could be historically much weaker. But it seems that to find many more  $\gamma$ -ray-emitting blazars with radio fluxes lower than  $\sim 0.5$  Jy at 5 GHz, the  $\gamma$ -ray detection limit would have to be much lower than what EGRET can provide.

## RADIO STATE FOR $\Gamma$ -RAY EMISSION

From the studies of Reich et al. [12], Mücke et al. [13], Valtaoja et al. [14], Pohl et al. [15], Lähteenmäki et al. [16], and Marscher et al. [17,18], opinions now all seem to converge to the picture that: (1) higher the radio activities are, more often high-energy  $\gamma$ -rays are detected; (2) high-energy  $\gamma$ -rays are most likely detected when the source is in the rising phase of a radio flare; (3) it is moderately likely when the radio flux is in a high-flux stage; (4) it is least likely when the source is in the declining phase of a flare. We must also mention, as described above, that the high-energy  $\gamma$ -ray flux is moderately correlated with the *increase* of radio flux at the time of the EGRET measurement, but not to the flare size itself [7]. This picture represents the current understanding of the radio state when an EGRET flux is detected. It points to the possibility that the high-energy  $\gamma$ -rays as detected by EGRET are most likely emitted in flares and the durations of  $\gamma$ -ray flares are much shorter than the radio flares. But it does not preclude the possibility that low-level continuous fluxes of high-energy  $\gamma$ -rays may also exist in blazars.

## RADIO MORPHOLOGY

Recently Piner and Kingham [19] published their VLBI study of six EGRET blazars and a number of blazars not detected by EGRET for comparison. Based

on their observations, they indicate that the  $\gamma$ -ray flares do not necessarily correlate with component ejections, (component ejections during  $\gamma$ -ray flares have been reported before; see e.g. Wehrle et al. [20]), the  $\gamma$ -ray blazars do not preferentially belong either to the population with misaligned jets or to the population without misaligned jets, and the  $\gamma$ -ray blazars are not found to be more strongly beamed than those which have not been detected by EGRET. In an ongoing VLBA monitoring program by Marscher et al. [17,18], with a large sample size and a long observation history, it has been found that about 50% of the observed radio flares are correlated with EGRET detections; the lack of detections in the other 50% can be explained with paucity of EGRET observations and brevity of  $\gamma$ -ray flares. Marscher et al. [17,18] also indicate that EGRET-detected blazars do show evidence of being more strongly beamed than those not detected by EGRET. This is at variance with what Piner and Kingham [19] find in this beaming question. But as pointed out by Piner [21], the measured average speed of EGRET sources, at  $6 h^{-1}c$ , by Piner and Kingham [19], is very similar to the value obtained by Marscher et al. [17,18]. The difference lies in the choice of objects for the sample of blazars not detected by EGRET. Marscher's sample [17,18] contains more recent results. We can perhaps draw a tentative conclusion for the beaming question at this time that EGRET-detected blazars are indeed more strongly beamed on the average than those not detected by EGRET.

## REFERENCES

1. Fichtel, C. E., *ApJS* **94**, 551 (1994).
2. Thompson, D. J., et al., *ApJS* **101**, 259 (1995).
3. Hartman, R. C., et al., *ApJS* **123**, 79 (1999).
4. Mattox, J. R., et al., *ApJ* **481**, 95 (1997).
5. Mücke, A., et al., *A&A* **320**, 33 (1997).
6. Michelson, P. F., these proceedings.
7. Valtaoja, E., et al., *Proc. Heidelberg Work. on  $\gamma$ -Ray Emitt. AGN*, p.121 (1996).
8. Sreekumar, P., et al., *ApJ* **464**, 628 (1996).
9. Nolan, P. L., et al., *ApJ* **459**, 100 (1996).
10. Dingus, B. L., et al., *ApJ* **467**, 589 (1996).
11. Lin, Y. C., et al., *ApJS* **105**, 331, (1996).
12. Reich, W., et al., *A&A* **273**, 65 (1993).
13. Mücke, A., et al., *A&AS* **120**, 541 (1996).
14. Valtaoja, E., et al., *A&AS* **120**, 491 (1996).
15. Pohl, M., et al., *A.S.P. CONF. SER.* **110**, p.268 (1996).
16. Lähteenmäki, A., et al., these proceedings.
17. Marscher, A. P., et al., these proceedings.
18. Marchenko, S. G., et al., these proceedings.
19. Piner, B. G., and Kingham, K. A., *ApJ* **507**, 706 (1998).
20. Wehrle, A. E., et al., *Astroparticle Phys.* **11**, 169 (1999).
21. Piner, B. G., private communication.



# GeV outbursts in Mrk 501

P. Sreekumar\*, D. L. Bertsch\*\*, S. D. Bloom†, R. C. Hartman\*\*, Y. C. Lin††, R. Mukherjee‡, D. J. Thompson\*\*

\**ISRO Satellite Center, Bangalore, India*

\*\**NASA/Goddard Space Flight Center, Code 661, Greenbelt MD 20771*

†*Hampden-Sydney College, Hampden-Sydney, VA 23943*

††*W. W. Hansen Experimental Physics Laboratory, Stanford University, Stanford, CA*

‡*Barnard College and Columbia University, New York, NY 10027*

**Abstract.** Mrk 501 is the third TeV blazar with a known GeV component. Previous multiwavelength campaigns on Mrk 501 showed well correlated outbursts at x-ray and TeV energies with no significant activity at GeV energies. We present here new evidence suggesting GeV outbursts in Mrk 501 when the spectrum appears to be extremely hard. However, this outburst appears uncorrelated with emission at x-ray energies. The resulting spectral energy distribution suggests a sharp cut off in the high-energy emission beyond a few hundred GeV.

## I INTRODUCTION

Observations by the high-energy telescope EGRET on board the Compton Observatory have shown the presence of a class of active galactic nuclei called blazars that emit strongly in  $\gamma$ -rays (Mukherjee *et al.* 1997). Blazars are characterized by flat radio spectra ( $\alpha > 0.5$ ) and rapid time variability at most wavelengths. The  $\gamma$ -ray luminosity in blazars often dominate the bolometric luminosity, especially during outbursts. The third EGRET catalog (Hartman *et al.* 1999) lists 66 active galactic nuclei, of which 43 are clearly classified as flat-spectrum radio quasars (FSRQ), 16 as BL Lac objects (XBLs=2 and RBLs=14) and 7 belonging to a less well-defined category of sources (intermediate spectrum/radio sources). The catalog covered the Observatory phases (1–4) and does not include Mrk 501, since it was clearly detected only during phase 5 observations.

The discovery of nearby XBLs at TeV energies has reinvigorated  $\gamma$ -ray studies of these objects. Mrk 421, at a  $z$  of 0.031 is the closest BL Lac object seen at GeV energies and was the first discovered TeV blazar (Punch 1992). Gaidos (1996) reported the discovery of extremely short bursts at TeV energies in this source with doubling times of the order of 1 hour or less. Such short variability timescales strongly constrain possible emission mechanisms. A 30-minute burst when the TeV flux increased by a factor of 25, suggests extremely small emission regions (a few light hours) if one uses light-travel time arguments. Observations show no clear evidence for spectral variability during the flare. Correlated variability at x-ray energies suggests strongly the predominance of an inverse Compton process that scatters the soft photons (synchrotron or direct/scattered accretion disk photons) to higher energies. Unlike the dramatic variability seen at x-ray and keV energies, there is only a weak indication of an increase in 100 MeV - 10 GeV flux measured by EGRET during an outburst (Macomb 1995). PKS 2155-304 and Mrk 501 are the two other TeV blazars that have also been detected at GeV energies. PKS 2155-304 was first detected at GeV energies in phase 4 of CGRO (Vestrand, Stacy & Sreekumar 1995). Recently, this source was detected at TeV energies (Chadwick *et al.* 1998) during a  $\gamma$ -ray/x-ray high state (Sreekumar & Vestrand 1997; Vestrand & Sreekumar 1999). At a  $z$  of 0.1, PKS 2155-304 is the most distant TeV source detected to date and is an ideal candidate to study the intergalactic infra-red photons using the absorption signatures in the high-energy spectrum.

Mrk 501 at a  $z$  of 0.033, is the second closest BL Lac object known. It was discovered at TeV energies ( $E > 300$  GeV) by the Whipple group (Quinn 1996; Catanese 1997), the HEGRA Cherenkov telescope (Bradbury 1997; Aharonian 1997) and more recently by the Telescope Array Project (TAP) (Hayashida 1998). Mrk 501 also shows significant variability at x-ray, low-energy  $\gamma$ -ray and TeV energies. This source was detected for the first time in the 100 keV to 1 MeV range by OSSE, the resulting spectral energy distribution (SED) showing this emission to be most likely of synchrotron origin. This represents the largest extension of the synchrotron spectrum in any blazar to date. More importantly, the shift in the synchrotron cutoff energy from about 1 keV in the quiet phase to about 100 keV during the outburst, suggest an unprecedented increase in the maximum energy of the charged particle spectrum in the jet. Though initial analysis of the EGRET data showed no detection in the 100 MeV - 10 GeV range, recent analysis using observations in 1996 (Kataoka *et al.* 1999) reported a  $\sim 4\sigma$  detection. In this paper, we present results on Mrk 501 showing convincing detection above 500 MeV and new evidence for  $\gamma$ -ray outbursts at GeV energies.

## II OBSERVATIONS AND ANALYSIS

EGRET observations of Mrk 501 are listed in Table 1. The spark-chamber was operated in the narrow FOV mode during observations after phase 4. MeV-GeV detection of the source is evident in viewing periods (VP) 516.5 and 519.0. The

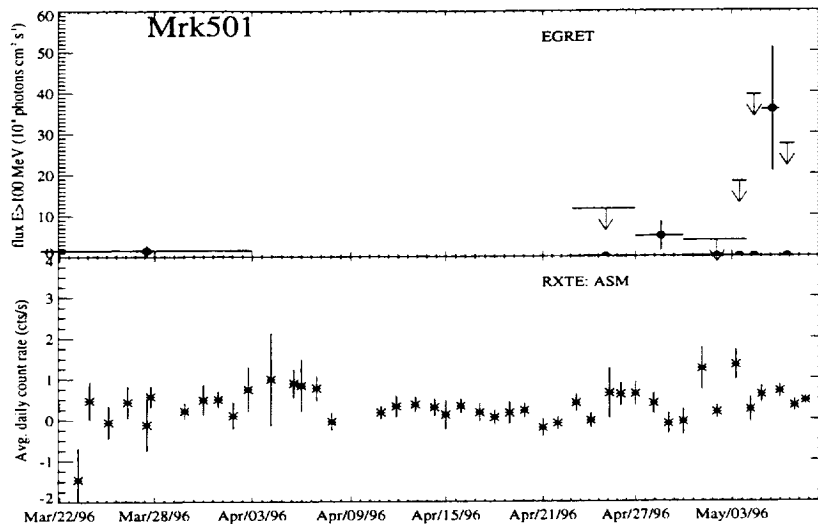


**FIGURE 1.** Time variability observed above 500 MeV (EGRET) and in the 2-12 keV band (ASM on RXTE). The  $\gamma$ -ray outbursts is uncorrelated with the x-ray emission.

strongest detection occurred during VP 519.0 ( $5.3\sigma$  above 500 MeV). A short time scale analysis (1-day) of the 2-week interval showed most of the source signal arrived within approximately a day (May 6 1996) (figure 1). Using photons that originate from within  $2^\circ$  of Mrk 501, a scatter plot of photon energy versus arrival time, showed 6 photons with energies  $>1$  GeV in  $\sim 1$ -day interval about May 6th (figure 2). The archival EGRET data yielded the mean expected rate from that region of the sky of  $\sim 0.19$  photons per day (from 6 weeks of exposure). This yields a  $<1e-6$  Poisson probability for detecting 6 GeV photons from the direction of Mrk 501 during 1-day. The EGRET sky exposure was also examined on a sub-hour time scale to determine any significant variations that could simulate an outburst and none was found.

### III RESULTS AND DISCUSSION

Careful analysis of EGRET data shows a clear detection of emission from Mrk 501 above 500 MeV where the much improved angular resolution makes the positional identification more certain. The unique synchrotron spectrum which sometimes extends to 100 keV implies that the inverse Compton emission peaks well beyond the EGRET energy range. This may explain why Mrk 501 was not detected as a strong GeV source during most EGRET observations even during x-ray/TeV outbursts. The new results presented here shows the first evidence for significant GeV emission from Mrk 501 that varies sharply over a time interval of 1-day or more. The GeV spectrum during this outburst (figure 3) is poorly determined (index =  $1.1 \pm 0.5$ )

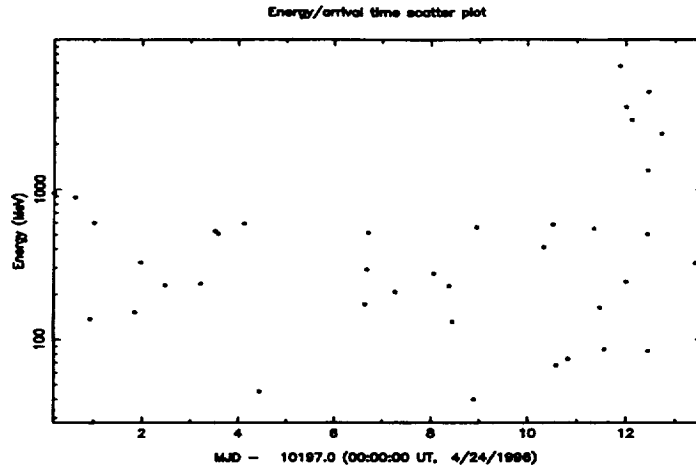


**FIGURE 2.** Photon energy vs. arrival time in the EGRET spark-chamber from a  $2^\circ$  region around Mrk 501. The GeV photons arrive mostly within a 24-hr interval on May 6 '99.

due to the limited statistics; however it shows the hardest known  $\gamma$ -ray spectrum in blazars. Previous correlated observations of Mrk 501 have shown nearly simultaneous outbursts at x-ray and TeV energies. Our search for multiwavelength data on Mrk 501 for May 6 yielded only 2–12 keV ASM data from the RXTE satellite. Figure 1 compares the ASM count rate with the EGRET measurements. No increase in the x-ray emission correlated with the GeV outburst is observed. Figure 3 shows the mean TeV spectrum (index =  $2.47 \pm 0.07$ ) published earlier by Aharonian *et al.* (1997). Though recent CAT results (Djannati-Atai *et al.* 2000) have suggested changes in the TeV spectrum for different intensity states of Mrk 501, the GeV spectrum suggests a break at  $\sim 100$  GeV. Alternately, using the observed correlation between x-ray and TeV emission from earlier outbursts, the ASM data can be used to set approximate upper limits on the TeV emission on May 6. The derived upper limit of  $1 \times 10^{-18}$  ergs/cm<sup>2</sup>-s-keV at 0.5 TeV, also requires the GeV

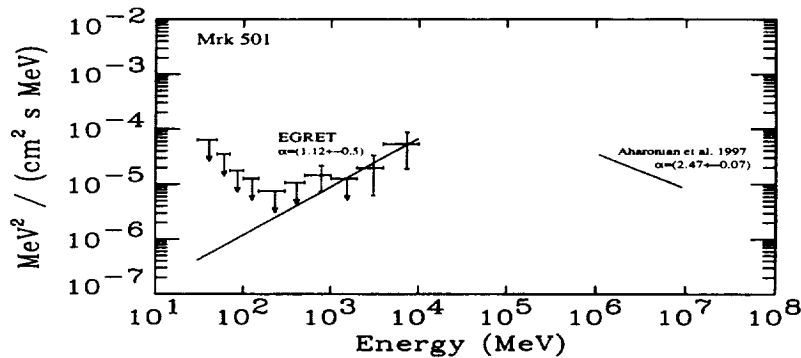


**FIGURE 3.** High-energy spectrum of Mrk 501. The non-simultaneous average TeV spectrum (Aharonian *et al.* 1997) suggests a break in the spectrum at  $\sim 100$  GeV

spectrum to break sharply around  $\sim 100$  GeV.

A likely scenario to explain the GeV outburst is a fresh injection of soft IR/optical photons that are Compton upscattered into the GeV range. However, preliminary analysis using standard SSC models (Bloom, private comm.) indicates difficulties in incorporating the derived TeV upper limit given the extremely hard GeV spectrum. It is unfortunate that no ground-based optical/IR data are available during the outburst in order to validate this. The exact nature of GeV outbursts in Mrk 501 maybe resolved only after the launch of the GLAST mission.

## REFERENCES

1. Aharonian, F., *et al.* 1997, A&A, 327, L5
2. Bradbury, S.M., *et al.* 1997, A&A, 320, L5
3. Catanese, M., *et al.* 1997, ApJ, 487, L143
4. Chadwick, P., *et al.* 1998, ApJ, 503, 391
5. Djannati-Atai, A., *et al.* 2000, AIP Conf. Proc. (this issue).
6. Gaidos, J.A., *et al.* 1996, Nature, 383, 319
7. Hartman, R.C., *et al.* 1999, ApJS, 123, 79
8. Hayashida, N., *et al.* 1998, astro-ph/9804043
9. Kataoka, J., *et al.* 1999, ApJ (in press).
10. Macomb, D.J., *et al.* 1995, ApJ, 449, L99
11. Mukherjee, R., *et al.*, 1997, ApJ, 490, 116
12. Punch, M., *et al.* 1992, Nature, 358, 477
13. Quinn, J., *et al.* 1996, ApJ, 456, L83
14. Sreekumar, P. & Vestrand, W.T. 1997, IAU Circular 6774
15. Vestrand, W.T., Stacy, G. & Sreekumar, P. 1995, ApJ, 454, L93
16. Vestrand, W.T., & Sreekumar, P. 1999, Astroparticle Phys. 11, 197

TABLE 1. EGRET Observations of Mrk 501 ( $E > 0.5$  GeV).

VP	Start	Stop	Flux	err	$\sigma$	Aspect
9.5 <sup>b</sup>	09/12/91	09/19/91	<11		0.0	3.4°
201.0 <sup>b</sup>	11/17/92	11/24/92	9	6	1.7	2.5°
202.0 <sup>b</sup>	11/24/92	12/01/92	8	7	1.1	5.8°
516.5	03/21/96	04/03/96	1.5	1.2	2.0	3.1°
519.0	04/23/96	04/27/96	3.75	3.16	1.6	1.23°
	04/27/96	04/30/96	4.93	3.60	2.1	
	04/30/96	05/04/96	<3.88		0.0	
	05/04/96	05/05/96	<39.4		1.6	
	05/05/96	05/06/96	35.85	15.15	5.3	
	05/06/96	05/07/96	<27.3	0.0	1.3	
617.8	04/09/97	04/15/97	2.13	1.74	1.9	3.0°

<sup>a</sup>flux in  $10^{-8}$  photons  $(\text{cm}^2\text{-s})^{-1}$ ; <sup>b</sup> $E > 100$  MeV flux

<sup>a</sup>



# Spectral Modeling of the EGRET 3EG Gamma Ray Sources Near the Galactic Plane

D.L. Bertsch<sup>1</sup>, R.C. Hartman<sup>1</sup>, S.D. Hunter<sup>1</sup>, D.J. Thompson<sup>1</sup>, Y.C. Lin<sup>2</sup>,  
D.A. Kniffen<sup>3</sup>, G. Kanbach<sup>4</sup>, H.A. Mayer-Hasselwander<sup>4</sup>, O. Reimer<sup>4</sup>, and  
P. Sreekumar<sup>5</sup>

1. Code 661, NASA/Goddard Space Flight Center, Greenbelt, MD 20771 USA
2. W. W. Hansen Exp. Phys. Lab., Stanford Univ., Stanford, CA 94305 USA
3. Code S, NASA Headquarters, 300 E. St. SW, Washington, DC 20024
4. Max-Planck Institut fur Extraterrestrische Physik, Giessenbachstr.  
D-85748, Garching, Germany
5. ISRO Satellite Center, Bangalore, India

**Abstract.** The third EGRET catalog lists 84 sources within  $10^\circ$  of the Galactic Plane. Five of these are well-known spin-powered pulsars, 2 and possibly 3 others are blazars, and the remaining 74 are classified as unidentified, although 6 of these are likely to be artifacts of nearby strong sources. Several of the remaining 68 unidentified sources have been noted as having positional agreement with supernovae remnants and OB associations. Others may be radio-quiet pulsars like Geminga, and still others may belong to a totally new class of sources. The question of the energy spectral distributions of these sources is an important clue to their identification. In this paper, the spectra of the sources within  $10^\circ$  of Galactic Plane are fit with three different functional forms; a single power law, two power laws, and a power law with an exponential cutoff. Where possible, the best fit is selected with statistical tests. Twelve, and possibly an additional 5 sources, are found to have spectra that are fit by a breaking power law or by the power law with exponential cutoff function.

## INTRODUCTION

The gamma ray sources near the Galactic Plane are likely to be from a more than one class of objects that are associated with our Galaxy. The spectral properties of these sources may offer a distinction between different source mechanisms. The five known pulsars for example exhibit relatively hard spectra and all except the Crab break at high energies. This paper examines the spectral properties of the EGRET third catalog (Hartman et al. 1999) sources within  $\pm 10^\circ$  of the Galactic plane.

## ANALYSIS

Each source in the EGRET Third Catalog (Hartman et al., 1999) was fitted with three functional forms, a single power law, two matching power laws, and a power law, modified by an exponential cut-off as shown in the following equations;

$$\frac{\partial J}{\partial E}(E, K, E_0, \lambda) = K \left( \frac{E}{E_0} \right)^{-\lambda} \quad (1)$$

$$\begin{aligned} \frac{\partial J}{\partial E}(E, K, \lambda_1, \lambda_2) &= K \left( \frac{E}{1000 \text{ MeV}} \right)^{-\lambda_1} && \text{for } E \leq 1000 \text{ MeV} \\ &= K \left( \frac{E}{1000 \text{ MeV}} \right)^{-\lambda_2} && \text{for } E \geq 1000 \text{ MeV} \end{aligned} \quad (2)$$

$$\frac{\partial J}{\partial E}(E, K, \lambda, E_f) = K \left( \frac{E}{300 \text{ MeV}} \right)^{-\lambda} \exp(-E/E_f) \quad (3)$$

In eq. 1,  $E_0$  was set to the value determined by the EGRET Spectral program to minimize the correlation between the two other fit parameters. The location of the break energy in eq. 2 was set to 1000 MeV to keep the number of parameters at a minimum since at best, there are only 10 energy points available. With each fit, a reduced  $\chi^2$  was obtained, and an F-Test was done to see if there is statistical justification in using either of the forms in eqs. 2 or 3 rather than a simple power law to fit the observed spectral data. In the F-Test, a value of  $P < 0.05$  is generally taken as the point where the more complicated fit is warranted. Summed data sets for Phases 1 through 4 of the CGRO (Compton Gamma Ray Observatory) mission were used to maximize the statistics since the sources in the Galactic plane region of the sky do not show strong variability.

## RESULTS

Six sources that are listed in the third EGRET catalog are thought to be artifacts from residual emission in the wings of the PSF (Point Spread Function) from Vela (see Hartman et al., 1999). These were removed from consideration, and just the remaining 78 sources were modeled. The photon energy spectra of the majority of these 78 sources were found to be best represented by a simple power law whose index is given in the catalog paper (Hartman et al., 1999). However, 28 of these were judged to be too limited statistically at the extremes of EGRET's energy range to have a meaningful measure of a departure from a simple power law spectrum.

The F-Test analysis of the change in  $\chi^2$  between a simple power law and the more complex forms (eqs. 2 and 3) indicated that 12 sources have complex spectra. Another 5 sources that are weak statistically also may exhibit a curving or breaking form. Table 1 lists the results of the two-power law modeling of these 17 sources. The column labeled "Spectral Category" indicates by the "2P" designation the 5 sources that are best fit by a breaking power law. These are also shown in bold in Table 1. The spectra of sources designated by "PE" are better described by power-law with an exponential cutoff. The sources labeled "SL" (shaded) are statistically limited and either model fits them reasonably well. The parameters of eq. 2 and their

Table 1. Two-Power-Law Fits to the EGRET Sources Within  $10^\circ$  of the Galactic Plane

Name	Type	Galactic		Spectral		Coefficient $10^{-11} \text{ cm}^{-2} \text{ s}^{-1}$	Index-1	Index-2	Red. $\chi^2$
		Long. deg.	Lat. deg.	Sigif. $\sigma$	Cat.				
3EG_J0617+2238	U	189.00	3.05	17.4	2P	$5.89 \pm 0.70$	$-1.79 \pm 0.09$	$-2.65 \pm 0.24$	0.91
3EG_J1710-4439	P	343.10	-2.69	21.4	2P	$16.71 \pm 9.08$	$-1.69 \pm 0.07$	$-2.26 \pm 0.13$	0.73
3EG_J1736-2908	U	358.79	1.56	5.8	2P	$7.15 \pm 1.67$	$-1.49 \pm 0.23$	$-5.80 \pm 1.39$	0.92
3EG_J1746-2851	U	0.11	-0.04	17.5	2P	$13.29 \pm 2.83$	$-1.20 \pm 0.27$	$-2.31 \pm 0.26$	2.64
3EG_J2021+3716	U	75.58	0.33	10.3	2P	$10.19 \pm 1.44$	$-1.23 \pm 0.15$	$-3.39 \pm 0.36$	0.55
3EG_J0633+1751	P	195.13	4.27	76.4	PE	$49.3 \pm 14.1$	$-1.38 \pm 0.07$	$-2.54 \pm 0.16$	7.51
3EG_J0834-4511	P	263.55	-2.79	73.8	PE	$107.6 \pm 40.2$	$-1.48 \pm 0.08$	$-2.50 \pm 0.19$	13.46
3EG_J1655-4554	U	340.48	-1.61	5.2	PE	$5.23 \pm 1.37$	$-1.44 \pm 0.26$	$-6.41 \pm 1.96$	0.38
3EG_J1741-2050	U	6.44	5.00	6.6	PE	$3.68 \pm 0.67$	$-1.71 \pm 0.16$	$-3.77 \pm 0.59$	0.62
3EG_J2020+4017	U	78.05	2.08	21.0	PE	$13.63 \pm 2.16$	$-1.87 \pm 0.10$	$-2.71 \pm 0.34$	2.60
3EG_J2027+3429	U	74.08	-2.36	5.8	PE	$2.55 \pm 0.75$	$-2.02 \pm 0.18$	$-20 \pm 20$	0.73
3EG_J2033+4118	U	80.27	0.73	11.8	PE	$7.72 \pm 2.50$	$-1.60 \pm 0.26$	$-3.85 \pm 1.29$	2.12
3EG_J0634+0521	U	206.18	-1.41	4.6	SL	$1.80 \pm 0.67$	$-1.56 \pm 0.37$	$-3.74 \pm 1.54$	0.55
3EG_J0747-3412	U	249.35	-4.48	3.5	SL	$2.23 \pm 0.66$	$-1.77 \pm 0.23$	$-21 \pm 21$	0.29
3EG_J1316-5244	U	306.85	9.93	5.7	SL	$1.43 \pm 0.34$	$-2.26 \pm 0.14$	$-19 \pm 19$	0.50
3EG_J1810-1032	U	18.81	-4.23	4.9	SL	$2.69 \pm 0.57$	$-1.98 \pm 0.15$	$-4.85 \pm 1.36$	0.42
3EG_J2206+6602	a	107.23	8.34	5.2	SL	$2.04 \pm 0.58$	$-1.99 \pm 0.20$	$-5.66 \pm 2.29$	0.34

Table 2. Power-Law-With-Exponential-Cutoff Fits to Sources Within  $10^\circ$  of the Galactic Plane

Name	Type	Galactic		Spectral		Coefficient $10^{-11} \text{ cm}^{-2} \text{ s}^{-1}$	Index	e-Folding Energy MeV	Red. $\chi^2$
		Long. deg.	Lat. deg.	Sigif. $\sigma$	Cat.				
3EG_J0633+1751	P	195.13	4.27	76.4	PE	$37.14 \pm 1.69$	$-1.29 \pm 0.06$	$2770 \pm 472$	4.24
3EG_J0834-4511	P	263.55	-2.79	73.8	PE	$80.61 \pm 4.14$	$-1.45 \pm 0.06$	$3807 \pm 925$	7.92
3EG_J1655-4554	U	340.48	-1.61	5.2	PE	$10.10 \pm 4.36$	$-0.27 \pm 0.63$	$299 \pm 111$	0.30
3EG_J1741-2050	U	6.44	5.00	6.6	PE	$4.97 \pm 0.80$	$-1.19 \pm 0.24$	$692 \pm 187$	0.36
3EG_J2020+4017	U	78.05	2.08	21.0	PE	$14.70 \pm 1.69$	$-1.78 \pm 0.13$	$2804 \pm 1428$	2.28
3EG_J2027+3429	U	74.08	-2.36	5.8	PE	$14.08 \pm 7.73$	$-0.81 \pm 0.47$	$234 \pm 85$	0.33
3EG_J2033+4118	U	80.27	0.73	11.8	PE	$15.07 \pm 6.87$	$-0.56 \pm 0.62$	$370 \pm 172$	1.69
3EG_J0617+2238	U	189.00	3.05	17.4	2P	$5.97 \pm 0.70$	$-1.68 \pm 0.15$	$2226 \pm 1003$	1.27
3EG_J1710-4439	P	343.10	-2.69	21.4	2P	$12.14 \pm 0.78$	$-1.75 \pm 0.07$	$8320 \pm 3914$	1.20
3EG_J1736-2908	U	358.79	1.56	5.8	2P	$10.42 \pm 3.90$	$-0.69 \pm 0.58$	$407 \pm 172$	1.02
3EG_J1746-2851	U	0.11	-0.04	17.5	2P	$7.02 \pm 1.74$	$-1.12 \pm 0.37$	$629 \pm 154$	0.61
3EG_J2021+3716	U	75.58	0.33	10.3	2P	$7.94 \pm 1.28$	$-0.63 \pm 0.30$		
3EG_J0634+0521	U	206.18	-1.41	4.6	SL	$23.3 \pm 11.3$	$-0.85 \pm 0.78$	$550 \pm 385$	0.48
3EG_J0747-3412	U	249.35	-4.48	3.5	SL	$60.7 \pm 46.5$	$-0.71 \pm 0.86$	$300 \pm 193$	0.36
3EG_J1316-5244	U	306.85	9.93	5.7	SL	$26.5 \pm 12.3$	$-2.20 \pm 0.38$	$201 \pm 163$	0.91
3EG_J1810-1032	U	18.81	-4.23	4.9	SL	$65.5 \pm 16.3$	$-1.30 \pm 0.27$	$473 \pm 139$	0.22
3EG_J2206+6602	a	107.23	8.34	5.2	SL	$67.6 \pm 28.8$	$-1.10 \pm 0.43$	$341 \pm 135$	0.19

uncertainties along with the reduced  $\chi^2$  value of the fit are given in Table 1.

Table 2 summarizes the fits using a power-law with an exponential cutoff form to the same 17 sources. There are 7 sources that are fitted best by this model. The fit parameters of eq. 3 are tabulated here.

Figure 1 compares the F-Test probability with the source significance. It is evident that most of the sources are near the significance threshold of  $5\sigma$  required of sources near the plane for inclusion in the third EGRET catalog. Some of the sources here are below the cutoff. They exceeded the Catalog threshold in either one viewing period or in some combination of viewing periods, but are not as strong in the Phase 1 through 4 data used here. Three pulsars, Vela, Geminga, and PSR 1706-44 (3EG-J1710-4439) below the dotted line and the Crab pulsar above the dotted line have the four highest significance levels in figure 1. Discounting these four sources, the remaining points have a source significance distribution that is similar to the points above the line (power-law spectra). In other words, there is not a significant bias for strong sources to have non-power law spectra.

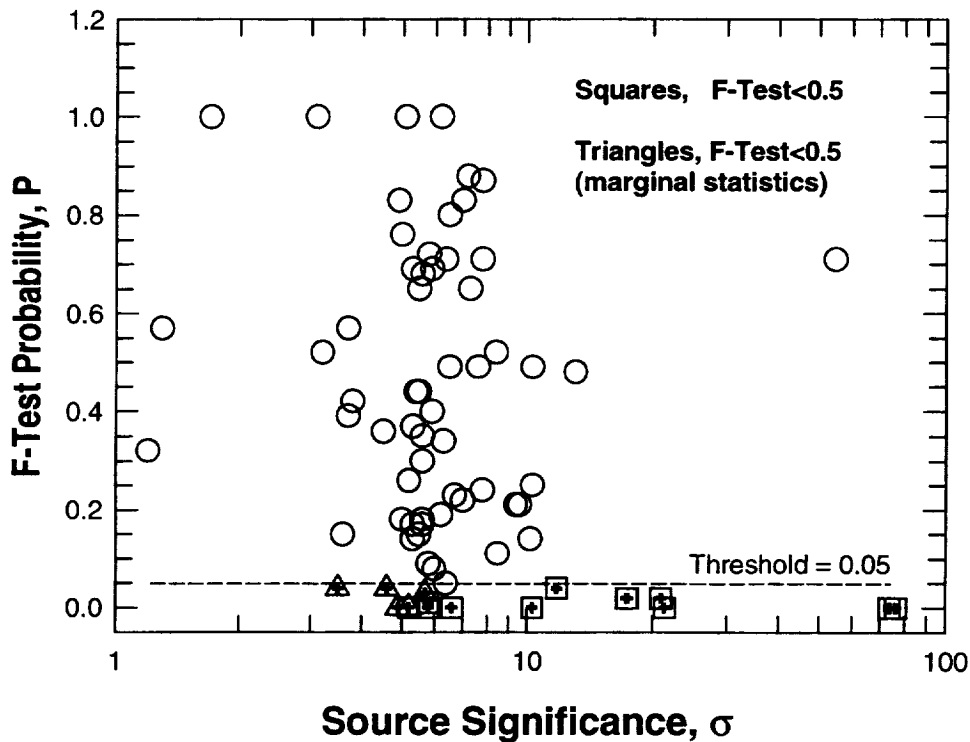


**FIGURE 1.** F-Test probability as a function of source significance. Points below the threshold line of  $P = 0.05$  are the sources that have spectra that are modeled best by a breaking power law or a power law with an exponential cutoff. The distribution with significance is similar for the sources above and below the dotted line if the four highest points (pulsars) are ignored.

## **CONCLUSIONS**

Among the sources within  $10^\circ$  of the Galactic Plane, at least 12 have spectral features that break at high energies. Three of these are known pulsars as noted above. The remaining 9 may be from a distinct class and perhaps are pulsar candidates themselves. EGRET will not be able to add significantly to the statistics on any of these sources, and it remains for the next generation gamma ray telescope, GLAST, to better determine their spectral features.

## **REFERENCES**

Hartman et al., 1999, ApJS, 123, 79.



# X-ray and $\gamma$ -ray Observations of the COS-B Field 2CG 075+00

R. Mukherjee\*, E. Gotthelf<sup>†</sup>, D. Stern\*, M. Tavani<sup>†+</sup>

\* *Dept. of Physics & Astronomy, Barnard College & Columbia University, NY, NY 10027*

<sup>†</sup> *Columbia Astrophysics Lab., Columbia University, NY, NY 10027*

+ *IFCTR-CNR, via Bassini 15, I-20133 Milano, Italy*

**Abstract.** We present a summary of  $\gamma$ -ray and X-ray observations of the intriguing COS-B field, 2CG 075+00, in order to search for potential counterparts. The third EGRET (3EG) catalog shows that the COS-B emission corresponds to at least two localized  $\gamma$ -ray sources, 3EG 2016+3657 and 3EG J2021+3716. We present analyses of archival X-ray fields which overlap error boxes of both the EGRET sources.

## INTRODUCTION

The EGRET (Energetic Gamma Ray Experiment Telescope) instrument on the Compton Gamma Ray Observatory (CGRO) has surveyed the  $\gamma$ -ray sky at energies above 100 MeV, detecting more than 270 point sources [4]. Of these, a large fraction ( $\sim 60\%$ ) remain unidentified, with no convincing counterparts at other wavelengths. Some of these unidentified sources were previously observed with the COS-B satellite, which carried out one of the first surveys of the  $\gamma$ -ray sky [14]. Surprisingly, only two of the unidentified COS-B sources have been subsequently associated with EGRET sources, and both are pulsars namely, Geminga [1], and 2CG 342-02 (PSR B1706-44) [15]. The nature of the unidentified  $\gamma$ -ray sources remains a long-standing mystery of high energy astrophysics.

In this article we re-visit the region containing the unidentified COS-B source 2CG 075+00, located in the Cygnus region, for which a significant amount of archival  $\gamma$ -ray (EGRET) and X-ray (ASCA & ROSAT) data have accumulated. Previous attempts to locate the origin of the high energy emission have been fraught with frustration, as the position associated with 2CG 075+00 in the second EGRET catalog [16], 2EG J2019+3719, has shifted significantly in the third EGRET catalog, and split between two nearby sources, 3EG 2016+3657 and 3EG 2021+3716. Fortunately, both revised EGRET error boxes have overlapping archival ASCA and ROSAT observations.

## I THE $\gamma$ -RAY OBSERVATIONS

2CG 075+00, first observed by COS-B, is located in the Galactic plane, at  $l = 75^\circ$ ,  $b = 0.0^\circ$ . The second COS-B catalog indicates an error radius of  $\sim 1.0^\circ$  for the source and notes that the source structure could possibly be interpreted as extended features [14]. The integrated  $\gamma$ -ray flux from the source was given to be  $1.3 \times 10^{-8}$  ph cm $^{-2}$  s $^{-1}$  although no spectral information was available.

Since its launch in 1991, EGRET has observed the error circle of 2CG 075+00 several times. Spatial analysis of the EGRET fields is performed by comparing the observed  $\gamma$ -ray map to that expected from a model of the diffuse Galactic and extragalactic radiation [5,12]. A maximum likelihood method is used to determine the source location and flux as a function of energy [7].

In the second EGRET (2EG) catalog, 2CG 075+00 was weakly detected as 2EG J2019+3719. Reanalysis of the region using a larger data set for the third EGRET catalog (3EG) revealed two sources, 3EG 2016+3657 and 3EG 2021+3716, located  $0.8^\circ$  away from the initial EGRET source. These more accurate, revised positions were derived from a likelihood analysis of the EGRET data for energies  $> 100$  MeV for the combined Phase 1 through Cycle 4 data (1991-1995) [4]. The two source positions have errors of  $33'$  and  $18'$ , respectively, at the 95 % contour.

Figure 1 shows the light curves of 3EG 2016+3657 and 3EG 2021+3716. The horizontal bars on the individual data points denote the extent of the viewing period for that observation. Fluxes have been plotted for all detections greater than  $2\sigma$ . For detections below  $2\sigma$ , upper limits at the 95% confidence level are shown. The flux levels of both the sources are roughly constant over the period of the EGRET observations, in contrast to that observed in blazars.

## II THE X-RAY OBSERVATIONS

Archival ROSAT and ASCA observations were available for both 3EG 2016+3657 and 3EG 2021+3716. The fields were of interest historically due to the presence

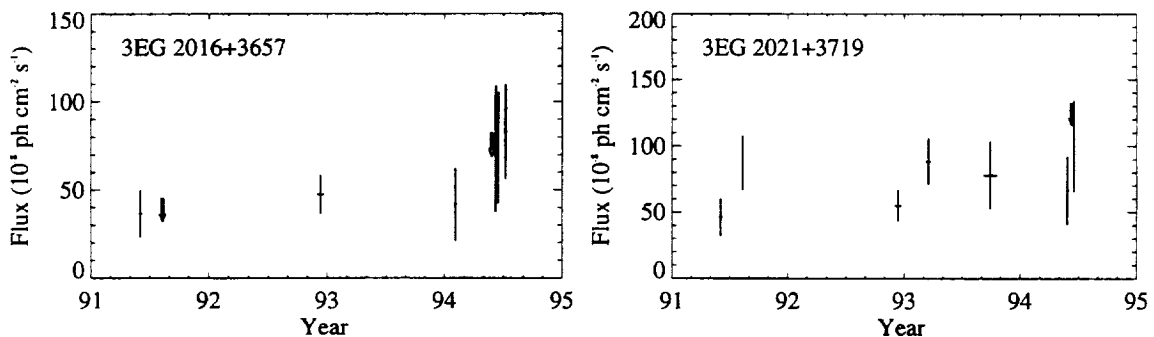


**FIGURE 1.** EGRET light curves for (a) 3EG 2016+3657 and (b) 3EG 2021+3716 from 1991 to 1995.  $2\sigma$  upper limits are shown as downward arrows.

of the 2CG source, as well as several other X-ray sources known to exist in the region. Two adjacent observations with ROSAT and ASCA fall nicely on the two 3EG error boxes.

We present data acquired with the ROSAT PSPC (Position Sensitive Proportional Counter) and the ASCA Gas Imaging Spectrometer (GIS) which allow complementary broad-band X-ray data in the 0.2 – 10 keV range with arcmin spatial resolution and moderate energy resolution. The PSPC 1° radius field-of-view is about twice that of the GIS. All data was obtained from the HEASARC archive at Goddard Space Flight Center and edited using the latest standard processing for each mission.

We created ROSAT and ASCA images of the region containing 3EG J2016+3657 and 3EG J2021+3716 by co-adding exposure corrected sky maps from each mission (see Fig. 2). These images are centered on the position of the earlier second EGRET catalog source, 2EG 2019+3716. However, the PSPC image size is large enough to include the 95 % error contours of both the 3EG sources, the positions of which are indicated with crosses. Note that the ASCA images are not centered on the EGRET positions, and only part of the 95 % error contour of 3EG 2016+3657 is covered by the ASCA observation.

The ROSAT maps were examined to search for a possible X-ray counterpart to the two 3EG  $\gamma$ -ray sources. The detected positions of X-ray sources in the ROSAT field are numbered in the image and are tabulated in Table 1. Several of these source are well known and were the target of the X-ray study.

The ASCA images were, similarly, searched for corresponding X-ray counterparts. No point sources were found in the ASCA image within the 95 % contour of 3EG

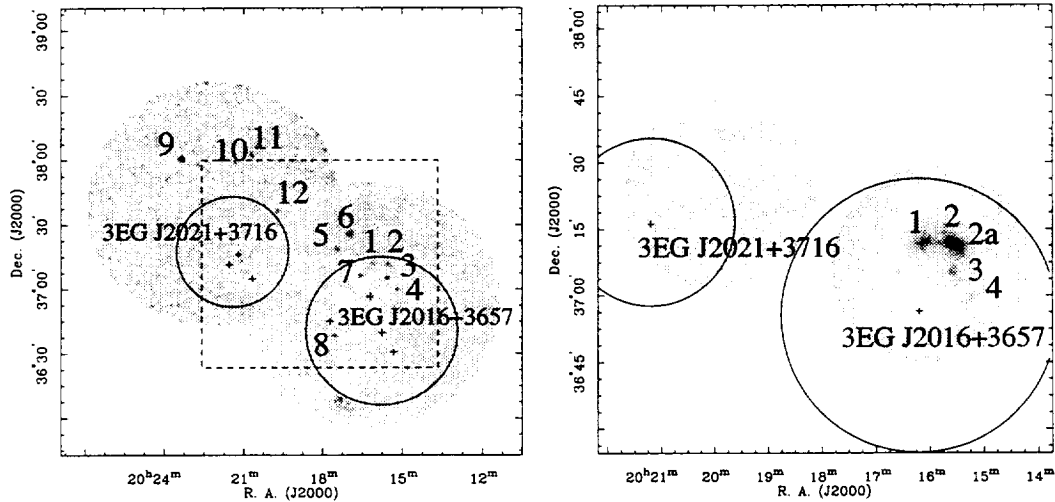


**FIGURE 2.** ROSAT (left) and ASCA (right) images of 3EG 2016+3657 and 3EG 2019+3719. The circles correspond to the 95% contours for the EGRET sources. The dashed rectangle in ROSAT image corresponds to the size of the ASCA image.

**TABLE 1.** X-ray sources in the ROSAT field of 3EG 2016+3657

Number <sup>a</sup>	Source Name	RA	Dec	Count Rate <sup>b</sup>	Other sources
1	CTB87	20 16 09.67	+37 12 17.5	24 ± 0.7	4C+37.57
2	1RXP J201534+3	20 15 34.57	+37 11 08.9	24 ± 0.7	1WGA J2015.5+3, 2E2013.7+370
3	2E2013.7+3655	20 15 38.52	+37 04 45.0	30 ± 0.7	
4	No counterparts			9 ± 0.6	
5	246	20 17 29.71	+37 18 31.3	3 ± 0.4	PPM 74637, SAO 69765
6	2E2015.1+3715	20 16 59.56	+37 25 18.6		1RXS J201700.4, HD193077 PPM 84624, SAO 69755
7	1WGA J2016.6+3	20 16 37.70	+37 05 53.8		
8	1WGA J2017.5+3	20 17 34.6	+36 38 06.6		1RXP J201736+3
9	1WGA J2023.3+3	20 23 21.70	+38 00 03.7		1RXP J202322+3
10	No counterparts				
11	1WGA J2020.7+3	20 20 43.30	+38 02 00.8		1RXP J202042+3
12	1WGA J2019.7+3	20 19 44.4	+37 35 44.8		

(a) Identifying number in ROSAT image (Fig. 2). (b) Source counts (ASCA) extracted from a 3 arcmin diameter aperture, in the 2-10 keV energy band and are background subtracted.

J2021+3716. The ASCA image of 3EG 2016+3657 revealed 5 point sources, as indicated with numbers in Fig. 2 (right). Source numbers 1, 2, 3 and 4 correspond to ROSAT sources of the same numbers in Fig. 2 (left). Source number 1 is coincident with the supernova remnant (SNR), CTB 87 (G74.9+1.2), that has a flat radio spectrum, with spectral index  $0.2 \pm 0.2$ . Table 1 gives the ASCA count rate for the four sources corresponding to the ROSAT sources. To measure the source count rate we extracted photons using a  $2'$  radius aperture and estimated the background contribution using a large annulus away from the other source following the method described in [3]. Source 2a in the ASCA image has no counterpart in the ROSAT image. We get an ASCA count rate of  $15 \pm 0.4 \times 10^{-3}$  for this source. Source 4 in the ROSAT and ASCA images appears to have no counterparts at other wavelengths. Further work on these sources is currently in progress, and will be presented elsewhere [9].

### III SUMMARY

We present a high energy study of the revised EGRET position of the intriguing COS-B field, 2CG 075+00, in order to search for possible X-ray counterparts. Neither of the two EGRET sources, 3EG 2016+3657 and 3EG 2021+3716, exhibit any significant evidence of variability, unlike for the typical EGRET blazar observation. No potential spectrally flat, radio-loud AGN counterparts exist for these sources.

In the past, efforts to identify the COS-B sources have included systematic multi-

wavelength observations. The field of 2CG 075+00 was mapped with the Effelsberg radio telescope at several frequencies [10], but no convincing counterparts were obtained.

It is interesting that no prominent X-ray source is in the gamma-ray error boxes considered here. Isolated gamma-ray pulsars at the distance of a few hundred parsecs might be consistent with both 3EG sources. Our study of archival X-ray (ASCA and ROSAT) data yields several faint sources within the error boxes of the two 3EG sources. The region contains tracers of star formation, several Wolf-Rayet stars, and OB associations. We notice the presence of the SNR CTB87 in the field of 3EG 2016+3657, a fact potentially quite important in light of the gamma-ray source/SNR associations noticed in previous investigations [13]. However, with the present data, given the large error boxes, it is not possible to argue in favor of any one source as the plausible counterpart to the EGRET sources.

Gamma-ray production from SNRs, Wolf-Rayet and OB associations is expected in several theoretical models, and our observations are a step towards the identification of a class of non-blazar unidentified gamma-ray sources near the Galactic plane. This subject was extensively investigated in the past for COS-B sources [8,17], and recently for EGRET sources [11,2,6]. Clearly, for the 3EG sources considered here, we need more refined gamma-ray positions and extensive monitoring (possibly by AGILE and GLAST) to establish their ultimate nature.

E.V.G.'s research is supported by NASA LTSA grant NAG5-7935. D.S. acknowledges support from the Hughes Grant at Barnard College.

## REFERENCES

1. Bertsch, D. L., et al. 1992, *Nature*, 357, 306.
2. Esposito, J. A., et al. 1996, *ApJ*, 461, 820.
3. Gotthelf, E. V. & Kaspi, V. 1998, *ApJ*, 497, L29.
4. Hartman, R. C., et al. 1999, *ApJS*, 123, 79.
5. Hunter, S. D., et al. 1997, *ApJ*, 481, 205.
6. Kaaret, P. & Cottam, J., 1996, *ApJ*, 462, 35L.
7. Mattox, J. R., et al. 1996, 461, 396.
8. Montmerle, T. 1979, *ApJ*, 231, 95.
9. Mukherjee, R., Gotthelf, E. V., & Tavani, M., in prep.
10. Ozel, M. E., et al. 1988, *A&A*, 200, 195.
11. Romero, G. E., Benaglia, P., & Torres, D. F. 1999, *A&A*, 348, 868.
12. Sreekumar, P., et al. 1998, *ApJ*, 494, 523.
13. Sturmer, S. J. & Dermer, C. D. 1995, *A&A*, 293, L17.
14. Swanenburg, B. N., et al. 1981, *ApJ*, 243, L69.
15. Thompson, D. J., et al. 1992, *Nature*, 359, 615.
16. Thompson, D. J., et al. 1995, *ApJS*, 102, 259.
17. Volk, H. J. & Forman, M. 1982, *ApJ*, 253, 188.



# Multiwavelength studies of the peculiar gamma-ray source 3EG J1835+5918

O. Reimer<sup>1</sup>, K.T.S. Brazier<sup>2</sup>, A. Carramiñana<sup>3</sup>,  
G. Kanbach<sup>1</sup>, P.L.Nolan<sup>4</sup>, D.J. Thompson<sup>5</sup>

<sup>1</sup> *Max-Planck-Institut für extraterrestrische Physik, 85740 Garching, Germany*

<sup>2</sup> *University of Durham, DH1 3LE Durham, England*

<sup>3</sup> *Instituto Nacional de Astrofísica Óptica y Electrónica, Tonantzintla, México*

<sup>4</sup> *W. W. Hansen Experimental Physics Lab, Stanford University, CA 94395 Stanford, USA*

<sup>5</sup> *LHEA Code 660, NASA GSFC, MD 20771, Greenbelt, USA*

**Abstract.** The source 3EG J1835+5918 was discovered early in the CGRO mission by EGRET as a bright unidentified  $\gamma$ -ray source outside the galactic plane. Especially remarkable, it has not been possible to identify this object with any known counterpart in any other wavelengths band since then. Analyzing our recent ROSAT HRI observation, for the first time we are able to suggest X-ray counterparts of 3EG J1835+5918. The discovered X-ray sources were subject of deep optical investigations in order to reveal their nature and conclude on the possibility of being counterparts for this peculiar  $\gamma$ -ray source.

## GAMMA-RAY OBSERVATIONS

EGRET observations of the unidentified  $\gamma$ -ray source 3EG J1835+5918 above 100 MeV in CGRO observation cycles 1 to 4 are covered in the Third EGRET catalog [1]. Moreover, 3EG J1835+5918 has been reported as a GeV  $\gamma$ -ray emitter [2], [3]. In order to obtain the most comprehensive data base on 3EG J1835+5918, we expanded the analysis up to the most recent EGRET observations (CGRO cycle 7). Viewing periods with 3EG J1835+5918 in the field of view were examined separately at energies above 100 MeV and above 1 GeV. As reported earlier [4], 3EG J1835+5918 was only seen by EGRET at large off-axis angle early in the mission, resulting in the indication of flux variability. The most recent variability study of EGRET sources above 100 MeV [5] restricts the off-axis location of any  $\gamma$ -ray source to be within  $25^\circ$ . Considering only nine periods matching this criterion, 3EG J1835+5918 was found to be constant within statistics. In order to acknowledge this approach, we label observations with up to  $25^\circ$  off-axis location different than observations outside  $25^\circ$ , see fig.1. The flux of 3EG J1835+5918 during the observations in cycle 7 (13-27 January 1998, aspect angle  $5^\circ$ ) can be evaluated by

considering a similar on-axis observation of Geminga during 7-21 July 1998. If we assume that the EGRET sensitivity has not changed appreciably between these observations and that Geminga remains a stable emitter in  $\gamma$ -rays as previously observed, we can derive an normalization for the flux of 3EG J1835+5918 in cycle 7. Figure 1 shows the resulting flux history of 3EG J1835+59 above 100 MeV throughout the EGRET mission.

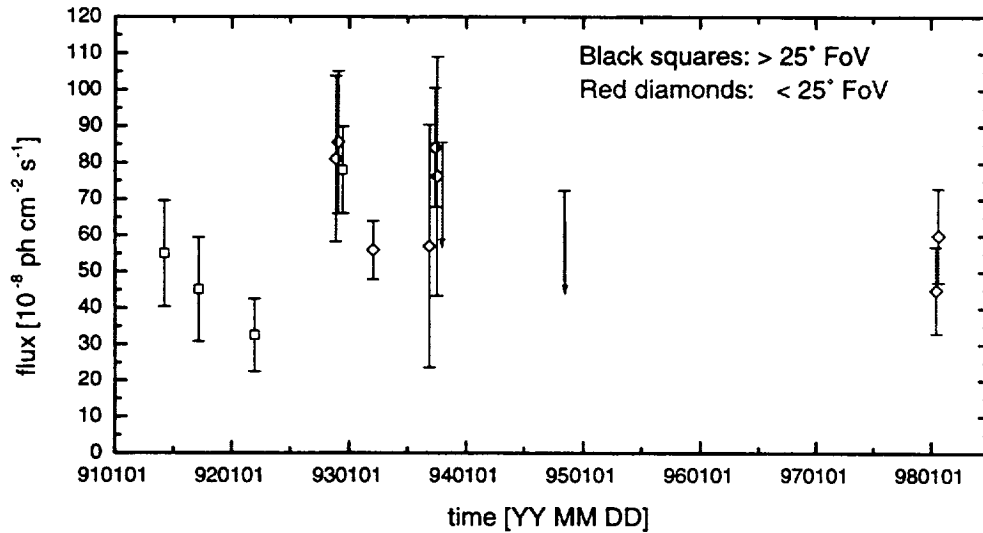


FIGURE 1. Flux history of EGRET observations on 3EG J1835+5918

The high-energy  $\gamma$ -ray spectrum is determined from EGRET observation of CGRO cycle 1 to 4. The power law spectral index is about -1.7 between 70 MeV and 4 GeV. Striking similarities to the  $\gamma$ -ray spectra of identified pulsars like Geminga and Vela can be seen in fig.2: the hard power law spectral index, a high-energy spectral cut-off or turnover and a low energy spectral softening.

The  $\gamma$ -ray source location is determined separately above 1 GeV using observations from cycle 1 to 7. Its precision (68% and 95% source location within a few arcminutes) allows us to cover the complete  $\gamma$ -ray error box with only one ROSAT HRI pointing. The  $\gamma$ -ray source confidence contours and the ROSAT HRI photon density is shown in fig.3.

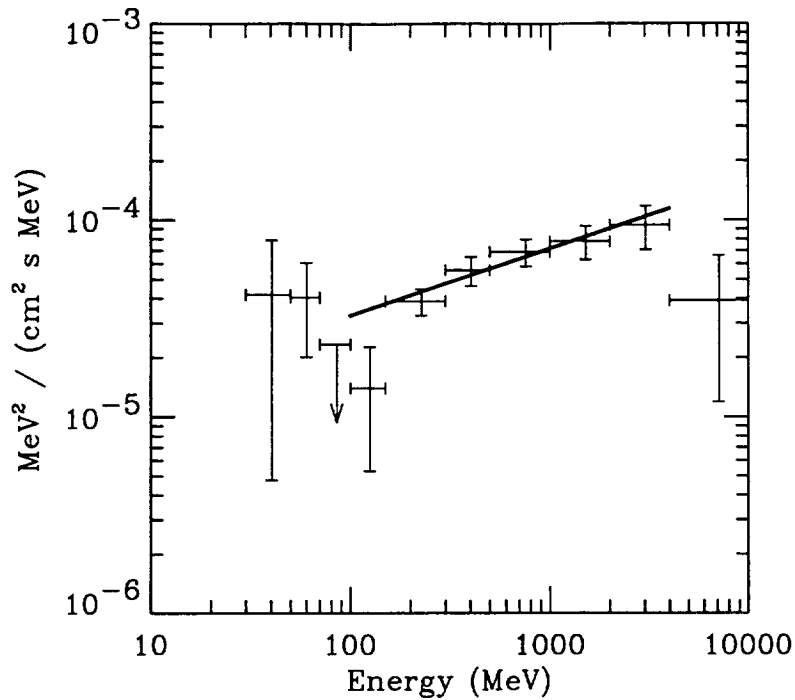


FIGURE 2. High energy gamma-ray spectrum of 3EG J1835+5918

## X-RAY OBSERVATIONS

With the 60 ksec ROSAT High Resolution Imager observation from December 1997/January 1998, the only previous HRI X-ray exposure of this source could be increased by a factor of 12. For the first time, we discovered point sources at X-ray energies between 0.1 and 2.4 keV. The sources are all faint with typical HRI count rates of  $1\text{-}3 \cdot 10^{-3} \text{ s}^{-1}$ . Two of the ten discovered sources are not in positional agreement with the determined  $> 1 \text{ GeV}$   $\gamma$ -ray source location contour, and therefore not considered as counterpart candidates. Using only ROSAT HRI data at this time, no spectral information on the discovered X-ray point sources is available.

## OPTICAL OBSERVATIONS

The discovered X-ray sources were subject of optical identification campaigns at the 2.12m telescope of the Observatorio Astrofísico Guillermo Haro (Cananea, México). A detailed description of the optical observations on 3EG J1835+5918 is presented elsewhere in these proceedings [6].

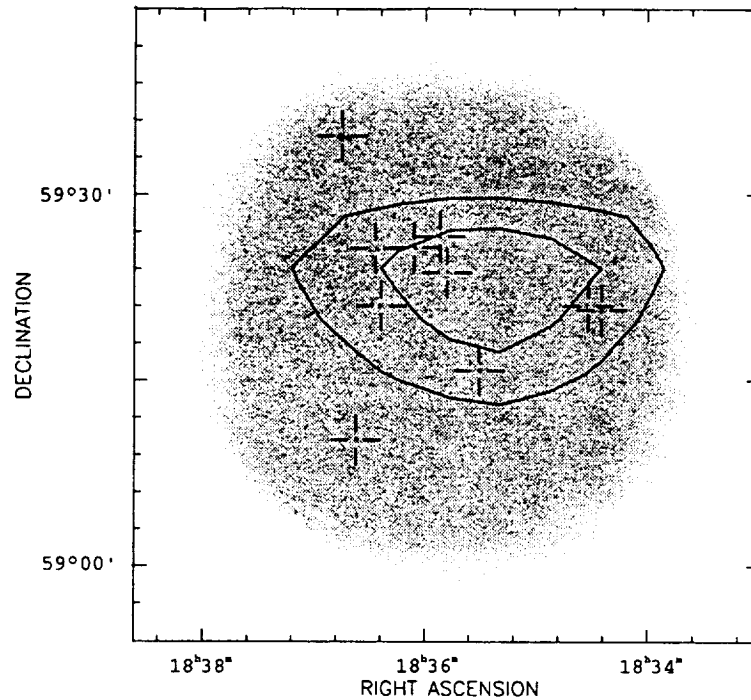


**FIGURE 3.** EGRET  $> 1$  GeV source location contours (68% and 95%) overlaid on the 60 ksec ROSAT HRI image

## RADIO OBSERVATIONS

Deep searches at radio wavelengths (770 MHz) at the position of 2EG J1835+59 have not detected any object above 0.5 Jy [7]. This result is in agreement with the correlation study between unidentified EGRET sources and catalogued flat-spectrum radio sources using the Green Bank 4.85 MHz and Parkes-MIT-NRAO 4.85 MHz surveys, which also did not find any counterpart for 2EG J1835+59 [8].

## SUMMARY & CONCLUSIONS

The brightest unidentified EGRET source at high galactic latitudes was subject of a multifrequency identification campaign. For the first time, counterparts in X-rays are suggested. The optical identification of the X-ray counterparts has been finished for the brighter sources [6], resulting in the elimination of four of the viable eight X-ray candidates. The eliminated X-ray sources are identified with stars or distant galaxies unlikely to be the  $\gamma$ -ray source. Spectra for the fainter candidates will have to be obtained at larger telescopes. This is currently in progress at the 6m telescope of the Special Astrophysical Observatory (Zelenchuk, Russia). The pulsar-like spectrum in  $\gamma$ -rays, the high-galactic latitude source location and the

lack of any blazar class object or flat spectrum radio source would suggest a nearby radio-quiet pulsar. Such pulsars are predicted [9] to exist among the unidentified  $\gamma$ -ray sources seen by EGRET. Perhaps the first ones were already found within the  $\gamma$ Cygni supernova remnant [10], the CTA1 SNR [11], with GeV J1417-6100 [12], and 2EG J0635+0521 [13]. We will conclude on the nature of this enigmatic  $\gamma$ -ray source when we will have completed the optical identifications of the remaining four weak X-ray sources coincident with 3EG J1835+5918.

## REFERENCES

1. Hartman, R.C. et al., *ApJS* **123**, 79 (1999)
2. Lamb, R.C. and Macomb, D.J., *ApJ* **488**, 872 (1997)
3. Reimer, O., Dingus, B. and Nolan, P.L., Proc. 25th ICRC, Vol.3, 97 (1997)
4. Nolan, P.L. et al., AIP Conf. Proc. 304, eds. Fichtel, C.E., Gehrels, N. and Norris, J.P., 361, (1994)
5. Tompkins, W., Ph.D. thesis, Stanford University, March 1999
6. Carramiñana, A. et al., these proceedings
7. Nice, D.J. and Sayer, R.W., *ApJ* **476**, 261 (1997)
8. Mattox, J.R., Schachter, J., Molnar, L., Hartman, R.C. and Patnaik, A.R., *ApJ* **481**, 95 (1997)
9. Yadigaroglu, I.-A. and Romani, R.W. *ApJ* **449**, 211 (1995)
10. Brazier, K.T.S., Kanbach, G., Carramiñana, A., Guichard, J., & Merck, M., *MNRAS* **281**, 1033 (1996)
11. Brazier, K.T.S., Reimer, O., Kanbach, G. & Carramiñana, A., *MNRAS* **295**, 819 (1998)
12. Roberts, M.S.E., Romani, R.W., Johnston, S., Green, A.J. *ApJ* **515**, 712 (1999)
13. Kaaret, P., Pirano, S., Halpern, J, Eracleous, M., *ApJ* **523**, 197 (1999)



# EGRET/COMPTEL Observations Of An Unusual, Steep-Spectrum Gamma-Ray Source

D. J. Thompson\*, D. L. Bertsch\*, R.C. Hartman\*, W. Collmar†, W. N. Johnson§

\*NASA/GSFC

†MPE

§NRL

**Abstract.** During analysis of sources below the threshold of the third EGRET catalog, we have discovered a source, named GRO J1400-3956 based on the best position, with a remarkably steep spectrum. Archival analysis of COMPTEL data shows that the spectrum must have a strong turn-over in the energy range between COMPTEL and EGRET. The EGRET data show some evidence of time variability, suggesting an AGN, but the spectral change of slope is larger than that seen for most gamma-ray blazars. The sharp cutoff resembles the high-energy spectral breaks seen in some gamma-ray pulsars. There have as yet been no OSSE observations of this source.

## INTRODUCTION

The construction of the third EGRET catalog (1) selected sources based on their statistical significance for the energy range  $E > 100$  MeV. After the catalog was completed, we investigated the possibility that some interesting steep-spectrum sources might have fallen below the catalog significance threshold. The strongest example of such a source is the one reported here. Its statistical significance in the summed maps from Phases 1-4 of the CGRO mission is highest in the energy band 50-70 MeV (over  $6\sigma$ ), while falling below  $4\sigma$  in the  $E > 100$  MeV energy range.

The position of this source is shown in the likelihood map of Figure 1. This map is constructed by combining likelihood maps from the 50-70, 70-100, and 100-150 MeV bands, where the source significance was highest. We define the best position by the centroid of the 95% confidence contour, and the uncertainty as the radius of this contour, as shown in the table below.

TABLE 1. Source Characteristics

Name	Gal. Long.	Gal. Lat.	R.A.	Dec.	95% radius
GRO J1400-3956	317.1°	21.0°	210.2°	-39.9°	1.3°

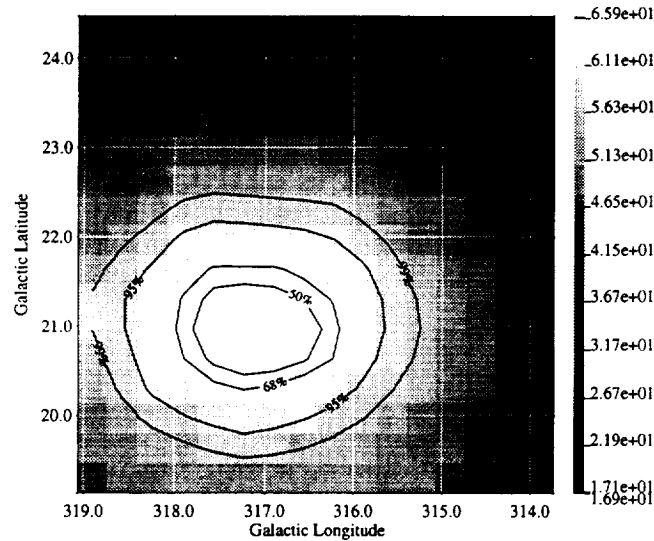


**FIGURE 1.** EGRET likelihood map for GRO J1400-3956 . The map represents a combination of maps for 50-70, 70-100, and 100-150 MeV for the summed Phases 1-4 data set. Third EGRET catalog sources were modeled (1).

## SIMULTANEOUS COMPTEL OBSERVATIONS

Because COMPTEL and EGRET are co-aligned on the Compton Observatory, and COMPTEL has a larger field of view than EGRET, GRO J1400-3956 was observable by COMPTEL in the same viewing periods as EGRET (primarily VP 0120, 0230, 0270, 2070, 2080, 2150, 2170, 3160, and 4240). For the map combining all the Phases 1-4 data, COMPTEL found little evidence for a source at the position identified by EGRET. Below 10 MeV, COMPTEL found only upper limits. In the 10-30 MeV band, COMPTEL's indication of a source was at the  $2\sigma$  level.

## SEARCH FOR COUNTERPARTS

At a Galactic Latitude of  $21^\circ$ , this source could be either Galactic or extragalactic. The Princeton pulsar catalog shows no pulsars within the error contours. The deeper pulsar survey now underway at Parkes covers this part of the sky and might offer new possibilities. The NASA Extragalactic Database (NED) shows many objects within this relatively large error box, but none that are obvious candidates to be the gamma-ray source: 15 galaxies, 8 IR sources, 8 weak radio sources, and several other objects. The brightest radio source, PKS 1402-388, has a 5 GHz flux density of only 0.25 Jy and a steep radio spectrum (-0.7), unlike the EGRET-detected blazars, which are typically brighter and have flat radio spectra.

One positional coincidence found in NED is with a gamma-ray burst, 3B940703B, whose error box is centered on celestial coordinates J1401-3911, well within the EGRET 95% error contour. Because the time of this burst was not during one of the

EGRET/COMPTEL pointings toward this direction, and both the EGRET and BATSE error boxes are relatively large, this is probably just a chance alignment.

Because this source is only about  $8^\circ$  from the core of radio galaxy Cen A, which has extended radio lobes, we checked for possible alignment of the source with the radio lobes. The new source is not aligned with the radio jets.

## ENERGY SPECTRUM

The EGRET detection of GRO J1400-3956 was strong enough in several energy bands to construct a spectrum. The data points and upper limits are consistent with a single power law with number index  $3.41 \pm 0.34$ . For every energy bin above 500 MeV, the likelihood test statistic is 0, showing no hint of emission at higher energies. This is one of the steepest source spectra seen by EGRET (see the paper by Bertsch et al. at this conference). If this spectrum extended unbroken into the COMPTEL band, it would be a bright COMPTEL source. The fact that COMPTEL has little evidence of the source indicates a strong change of slope.

In Figure 2, the COMPTEL limits and the one  $2\sigma$  excess (10-30 MeV) are combined with the EGRET data. In this case, the spectrum has been multiplied by  $E^2$ , giving the equivalent of a power per logarithmic energy interval. The dramatic change of spectral slope is obvious. The dotted line shows the extrapolation of the EGRET spectrum to lower energies. In order to be consistent with the data between 10 and 100 MeV, the change of slope must occur near 50 MeV (the EGRET 50-70 MeV point lies above the fitted line). Taking the slope above 50 MeV as the 3.4 index seen for

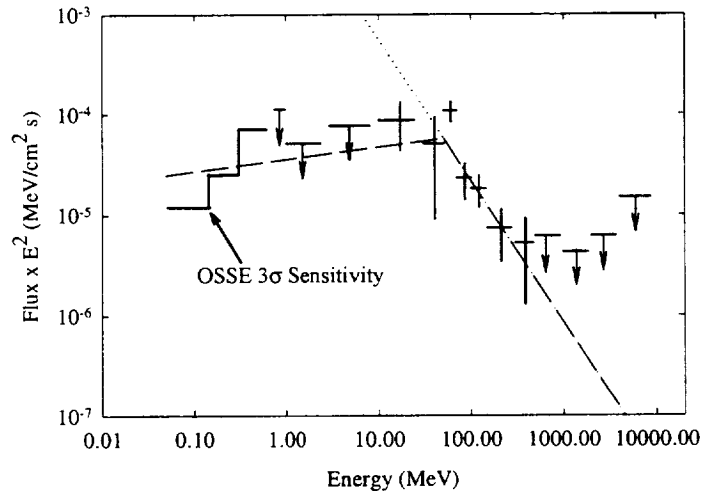


**FIGURE 2.** Energy spectrum of GRO J1400-3956, based on the sum of observations in Phases 1-4. Dotted line: power law fit to the EGRET data. Dashed line: broken power law consistent with the COMPTEL upper limits for the same observations. The histogram shows the OSSE  $3\sigma$  continuum sensitivity, although no OSSE observations have yet been done.

the EGRET data alone, the slope needed below 50 MeV in order to be consistent with the COMPTEL upper limits is 1.8, a change of 1.6 in index.

If the dashed line is the true spectrum, then OSSE should be able to detect the source. Conversely, an OSSE upper limit could further constrain the flattening seen below 50 MeV.

## TIME VARIABILITY SEARCH

The EGRET data were examined for time variability, using the 50-70 MeV band where the source is the brightest. The data show some, though not overwhelming, evidence of time variability of the source (Figure 3). In terms of the known EGRET sources, this behavior is more characteristic of AGN than of pulsars, although none of the known EGRET blazars show spectra as steep as this source.

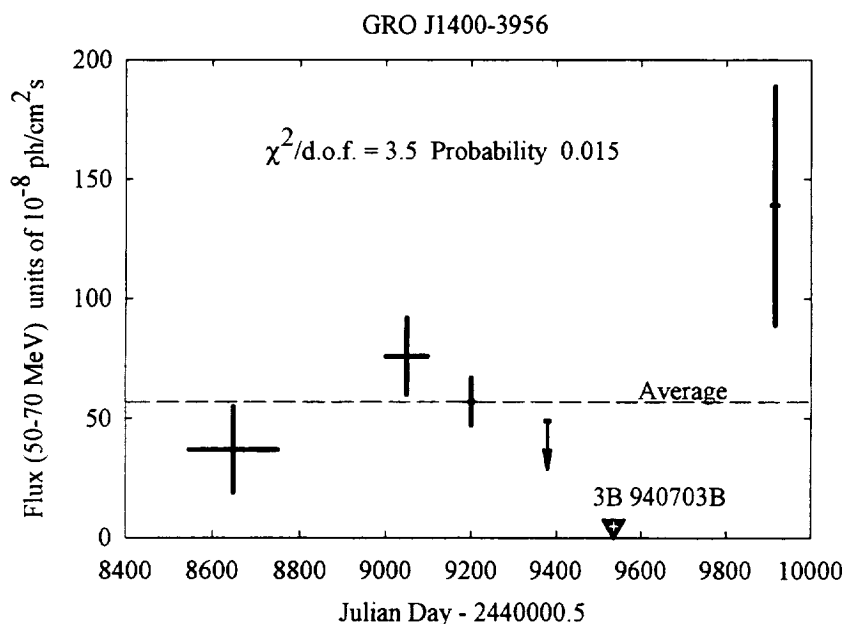


**FIGURE 3.** EGRET 50-70 MeV flux from GRO J1400-3956 during different observations. The dashed line shows the average from all EGRET data. The time of 3B940703B, from the same direction, is also shown.

## SUMMARY

The distinguishing feature of GRO J1400-3956 is the spectral shape with a strong change of slope near 50 MeV. Among the known gamma-ray sources, this feature is unique. Such a strong change of slope is not expected in most physical models involving accelerated particles, unless there is some sort of cutoff in the particle spectrum. The slope change most resembles the pulsar cutoffs seen in the GeV range for Vela and Geminga (2,3) or the spectral changes seen near 1 MeV for some "MeV-peaked" blazars.

This source represents a unique combination of features: a strong change in spectral slope near 50 MeV, a suggestion of time variability, and a lack of pulsar or blazar radio counterparts. Whether it represents an unusual example of a known class of gamma-ray sources or something entirely different remains an open question.

We continue to study GRO J1400-3956 with the Compton Observatory in two ways:

- There have been a number of COMPTEL observations of this sky region since the last useful EGRET observation (VP4240), because the source is often within the COMPTEL field of view during observations of Cen A or PSR B1509-58, both of which have been frequent COMPTEL targets. Preliminary analysis of these later COMPTEL observations has not yielded a strong detection, but the work is ongoing. These data might help clarify the spectrum and/or the possibility of time variability.
- A CGRO Cycle 9 proposal for additional COMPTEL observations and the first OSSE observations has been accepted. As shown in Figure 2, the OSSE data should either provide a detection or a further constraint on the spectral shape. The tentative scheduling shows the source being observed during the early part of 2001. Perhaps these observations will turn up a new gamma-ray surprise for the new Millennium.

In the longer run, the peak of the luminosity appearing in the 50 MeV range suggests that this will be a good candidate for observations with GLAST. With its much larger sensitivity and better angular resolution, GLAST should have the capability of shedding more light on this intriguing source.

## REFERENCES

1. Hartman, R.C. et al., *ApJS* **123**, 279-202 (1999).
2. Kanbach, G. et al., *A&A* **289**, 855-867 (1994).
3. Mayer-Hasselwander, H.A. et al., *ApJ* **421**, 276-283 (1994).



# Preliminary Results From A New Analysis Method For EGRET Data

D. J. Thompson, D. L. Bertsch, S. D. Hunter, P. Deines-Jones

*NASA/Goddard Space Flight Center*

B. L. Dingus

*University of Utah*

D. A. Kniffen

*Hampden-Sydney/NASA HQ*

P. Sreekumar

*ISRO Satellite Center*

**Abstract.** In order to extend the life of EGRET, the gas in the spark chamber was allowed to deteriorate more than was originally planned for the nominal two year Compton Observatory mission. Gamma ray events are lost because the pattern recognition analysis rules are not optimized for the poorer quality data. By changing the rules used by the data analysts, we can recover a significant fraction of the lost events, allowing improved statistics for detection and study of sources. Preliminary results from the Crab, Geminga, and BL Lacertae indicate the feasibility of this analysis.

## CONCEPT

In EGRET, each trigger produces a picture in the spark chamber, with examples shown in Figure 1. Although the hardware trigger rejects the vast majority of the charged-particle background EGRET encounters, the useful pictures currently represent fewer than 10% of the total triggers. The useful pictures are those for which there is clear evidence of a pair-production event within the spark chamber. EGRET analysis uses a pattern recognition program (with manual verification using selection rules) to select the useful pair-production events. These methods were derived and optimized empirically (1), based on accelerator calibration data.

The performance of EGRET has diminished due to deterioration of the spark-chamber gas. The older gas produces fewer real signals and more spurious sparks, as can be seen in Figure 1. This was planned for by including a gas replenishment

system. The five refills, planned to allow a two-year lifetime, have been stretched out to more than eight years. As a result, the detection efficiency for EGRET is now less than 25% of what it was at the beginning of the mission. Correction for this loss of efficiency has been done by comparing overlapping regions of the sky, taking the diffuse emission as a steady reference source within any region.

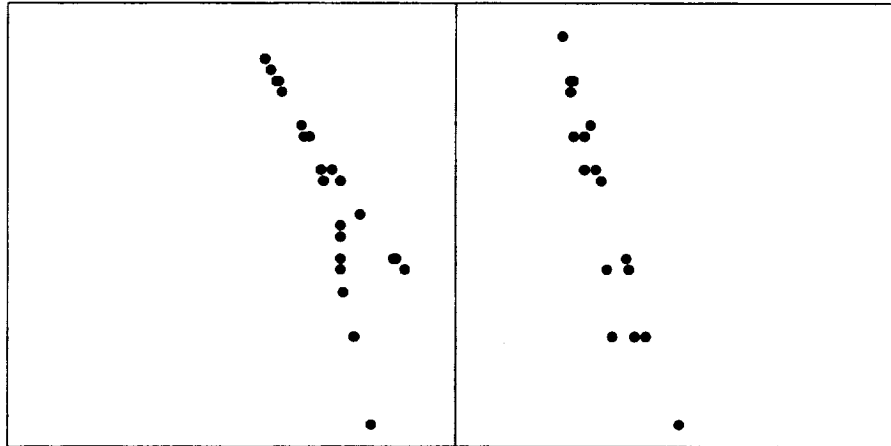


**FIGURE 1.** Left: gamma-ray pair event under good operating conditions. Right: gamma-ray pair event under poor operating conditions.

The principal motivation for this new analysis method is the fact that the hardware trigger for EGRET has not changed, only the ability of the pattern recognition program and the data analysts to accept events under the rules established when the instrument performance was much better. During periods of poorer EGRET performance there are nearly three times as many gamma rays in the EGRET data as appear in the final maps and event lists. Recovering “lost” events can substantially improve EGRET observations.

## PROCEDURE

Under CGRO Cycle 7 and Cycle 8 proposals, EGRET data analysts have reviewed several sets of events that were rejected by the standard data processing system, using new techniques:

- (1) We developed new selection criteria to screen sets of rejected events most likely to contain recoverable gamma rays.
- (2) The analysts processed events with the characteristic pair structure, but with gaps in the tracks, spurious sparks, or other defects that had caused the events to be rejected.
- (3) We processed these events for energy and direction, using software similar to that used for regularly-accepted events.

(4) Using a pointing toward the Galactic anticenter, we generated spectra for the bright Crab and Geminga pulsars using a combination of regular and “recovered” events. From these spectra, we derived sensitivity correction factors for each of the standard EGRET energy bands.

Even with the restricted selection criteria, a large number of events must be reviewed by the analysts; this is a labor-intensive process. With the limited budget, the number of experienced EGRET data analysts has decreased steadily, further slowing this review process. At present, we have only one full-time data analyst, who works on this recovery analysis part-time when not involved in regular data processing activities for current EGRET data.

## PROOF OF CONCEPT - GALACTIC ANTICENTER, VP 5280

The figures below show analysis of spatial, timing, and energy spectral data with the recovered events. Both the intensity map (Figure 2) and the pulsar light curve (Figure 3) show the same basic features as seen in the standard data analysis, demonstrating that the recovered events can be used to enhance statistics for gamma-ray sources. By comparing the energy spectra derived from the standard analysis with that from the combined standard + recovered data, we find that more events are recovered at lower energies. The correction factors needed to recover absolute flux values (Figure 4) are derived from a combination of the two source spectra (the Crab has a softer spectrum than Geminga; therefore the combination should give a correction applicable to all but the most unusual spectra).

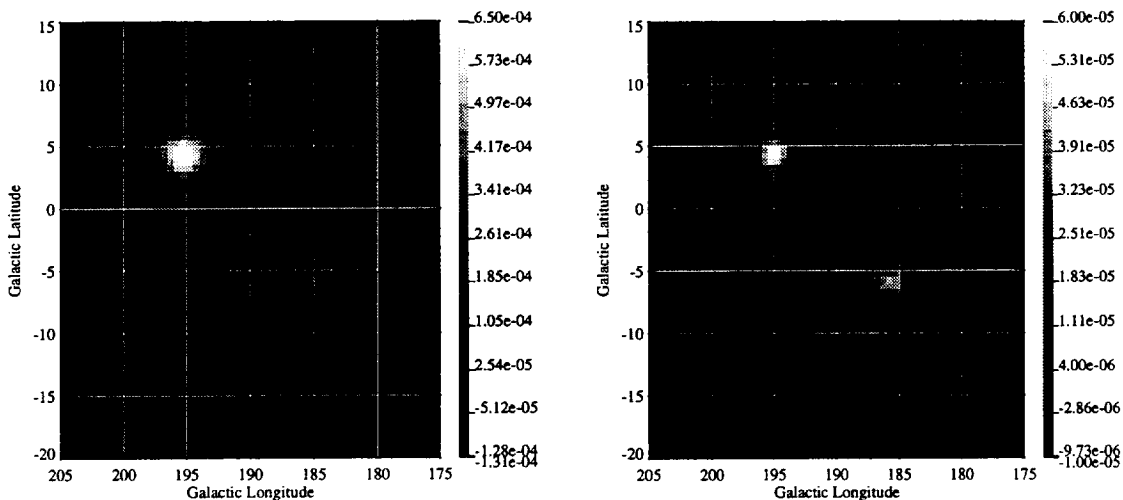


**FIGURE 2.** Left: Intensity map of the Galactic anticenter, VP5280, using standard analysis. Right: Intensity map of the Galactic anticenter, VP5280, using recovered event analysis. Note that the standard exposure has been used, so that the absolute intensity is not correct.

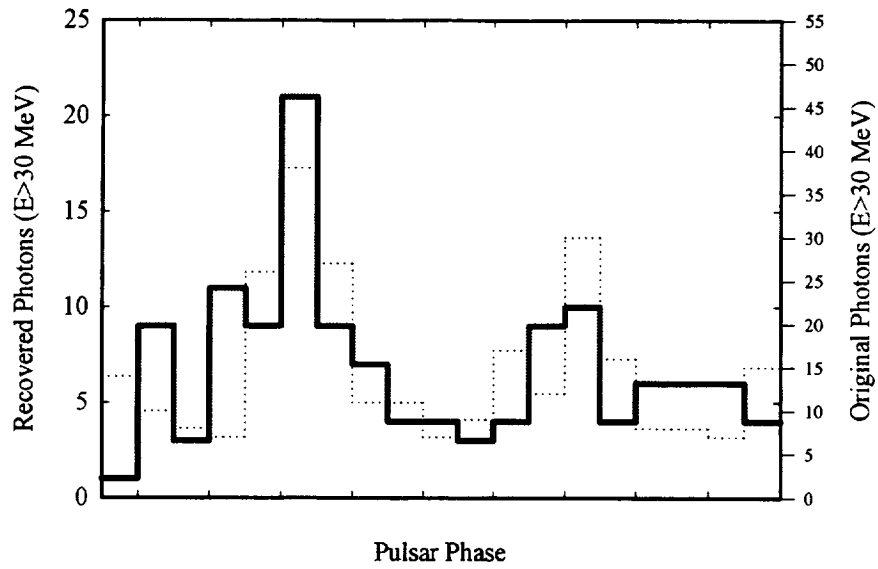


**FIGURE 3.** Light curve for the Crab pulsar. Solid line: recovered events only. Dotted line: standard events only. The two peaks of the typical Crab light curve are seen in both data sets, in phase.

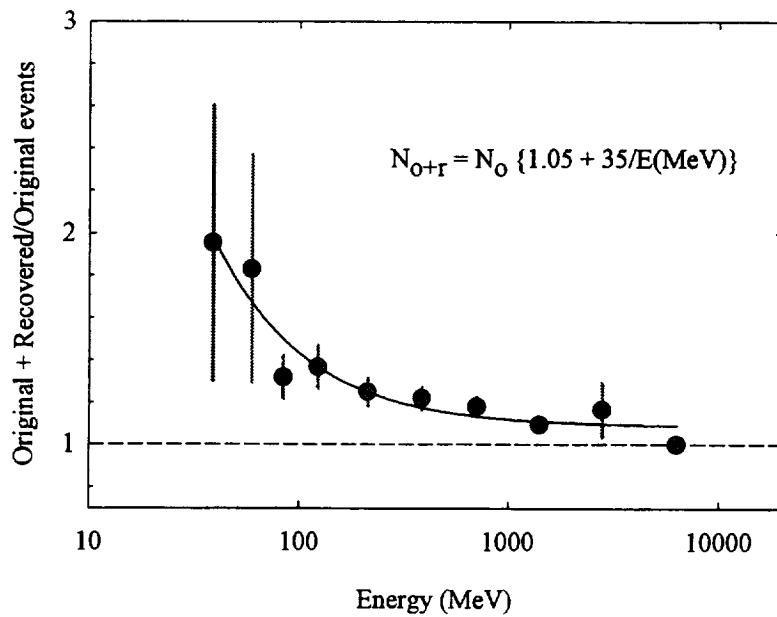


**FIGURE 4.** Energy-dependent correction factors for flux values that include recovered events compared to the original analysis. These factors are derived from the Crab and Geminga spectra measured in VP5280.

## AN EXAMPLE - THE SPECTRUM OF BL LAC, VP6235

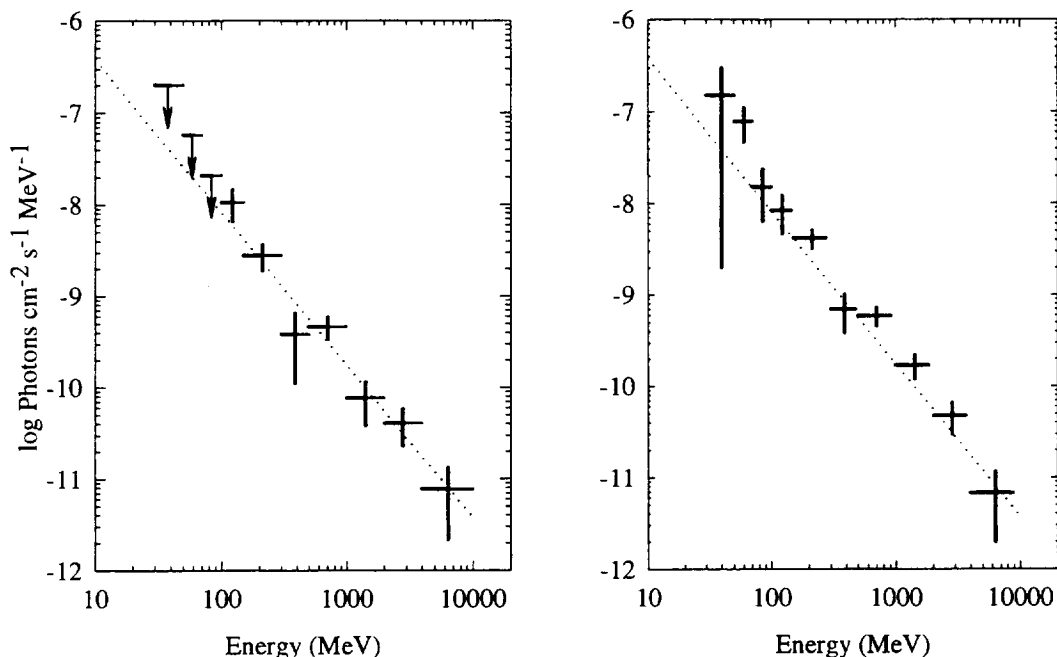


**FIGURE 5.** Left: BL Lac flare energy spectrum using original events only. Right: BL Lac flare spectrum using standard + recovered events. The flux in each energy bin has been scaled using the correction factors derived from the Crab/Geminga observation (Figure 4). The flux and power law index are consistent between the two spectra ( $1.68 \pm 0.16$  for the standard data,  $1.73 \pm 0.10$  for the enhanced data), but better measured with the addition of the recovered events, because the error bars are smaller and upper limits have been converted into detections at low energies. The consistency indicates that the corrections derived from the Crab and Geminga are reasonable.

The recovery technique was applied to the observation of the flare of BL Lacertae in VP 6235. The improved measurement of the spectrum (Figure 5) strengthens previous conclusions about this flare (2):

- The spectrum is significantly flatter during the flare than during the only previous EGRET detection of BL Lac.
- The spectrum is consistent with a single power law, showing no evidence for a change of slope or curvature as might be expected in some models (3).

## REFERENCES

1. Thompson, D.J. et al., *ApJS* **86**, 629-656 (1993).
2. Bloom, S.D. et al., *ApJ* **490**, L145-L148 (1997).
3. Madejski et al., *ApJ* **521**, 145-154 (1998).



# A Systematic Search for Short-term Variability of EGRET Sources

P. M. Wallace<sup>1</sup>, D. L. Bertsch<sup>2</sup>, S. D. Bloom<sup>3</sup>, N. J. Griffis<sup>1</sup>, S. D. Hunter<sup>2</sup>,  
D. A. Kniffen<sup>4</sup>, D. J. Thompson<sup>2</sup>

<sup>1</sup>*Department of Physics and Astronomy, Berry College, Mt. Berry, GA 30149*

<sup>2</sup>*NASA/Goddard Space Flight Center, Greenbelt, MD 20771*

<sup>3</sup>*IPAC, JPL/Caltech, MS 100-22, Pasadena, CA 91125*

<sup>4</sup>*Department of Physics and Astronomy, Hampden-Sydney College, Hampden-Sydney, VA 23943 and  
NASA HQ, Washington, DC 20546*

**Abstract.** The 3rd EGRET Catalog contains 170 unidentified high-energy ( $E > 100$  MeV) gamma-ray sources, and there is great interest in the nature of these sources. One means of determining sources class is the study of flux variability on time scales of days; pulsars are believed to be stable on these scales while blazars are known to be highly variable. In addition, previous work has led to the discovery of 2CG 135+01 and GRO J1838-04, candidates for a new high-energy gamma-ray source class. These sources display transient behavior but cannot be associated with any known blazars. These considerations have led us to conduct a systematic search for short-term variability in EGRET data, covering all viewing periods through cycle 4. Three unidentified sources show some evidence of variability on short time scales; the source displaying the most convincing variability, 3EG J2006-2321, is not easily identified as a blazar.

## INTRODUCTION

There are 271 sources listed in the 3rd EGRET Catalog of High-energy Gamma-ray Sources<sup>1</sup>. Besides one solar flare, the Large Magellanic Cloud, and a possible association with a radio galaxy (Cen A), the identified sources are distributed among two established classes of high-energy gamma rays: pulsars and radio-loud blazars. Pulsars are believed to not vary in gamma-ray output over time scales of one or two days, while blazars are known to be highly variable. While many instances of blazar flares have been reported, no comprehensive survey of EGRET data has been performed. It is the purpose of this study to conduct a systematic search for short-term variability in EGRET data from cycles 1-4. This paper focuses on the unidentified 3EG sources.

## DATA & ANALYSIS

All unidentified 3EG sources are examined across all viewing periods (VP's) for evidence of variability. The VP's are broken down into one-day intervals and intensity maps are generated for each day. With such short intervals, the statistics are extremely limiting; therefore this study is sensitive to only the strongest changes in gamma-ray

output. Only those light curves with at least one  $4\sigma$  one-day detection are considered for close analysis.

The remaining light curves are analyzed using the variability index  $V$ . If  $Q$  is the probability of obtaining a value of  $\chi^2$  equal to or greater than the empirical  $\chi^2$  from an intrinsically nonvariable source, then  $V \equiv -\log Q$ . All curves with  $V \leq 1.0$  are considered to be not variable. The curves are also inspected for evidence of flaring; those that display such evidence are modeled by Monte Carlo methods in order to determine the probability of finding such a flare from an intrinsically stable source. Three unidentified 3EG sources displayed  $V \geq 1.0$  and/or evidence of flaring. They are discussed below.

### 3EG J1410-6151

During the first four days of VP 14.0, the flux of 3EG J1410-6151 fell from  $(5.4 \pm 1.5) \times 10^{-6}$  photons  $\text{cm}^{-2}\text{s}^{-1}$  to below EGRET's sensitivity where it remained for the rest of the 14-day period; this is suggestive of flaring behavior. (See Figure 1.) Monte Carlo simulation gives a probability of 0.0007 that the fluctuation found in this VP is produced by a nonvariable source. It has been suggested<sup>2</sup> that 3EG J1410-6103 ( $l = 312.18$ ,  $b = -0.35$ ) is associated with SNR G312.4-0.4, which falls just outside the 68% error contour. It should be noted that although this VP occurred early in EGRET's life when its sensitivity was high, the source is  $27^\circ$  off-axis.

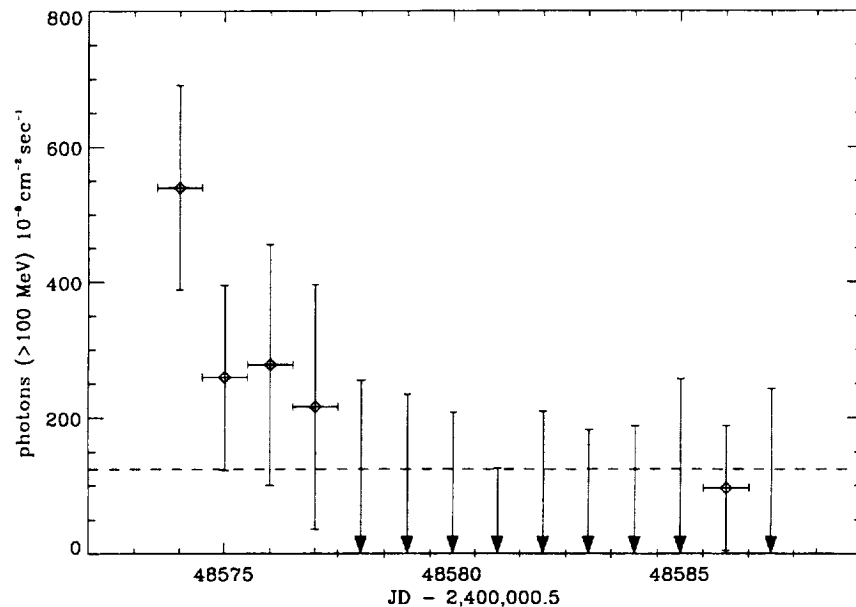


FIGURE 1. Light curve of 3EG J1410-6151 from VP 14.0.  $V = 1.47$ .

## 3EG J1746-2851

As this source is unidentified, strong, and coincident with the Galactic Center, it has been studied in some detail<sup>3</sup>. However, until now its short-term variability has not been examined, and there is some evidence of variability in VP's 16.0 and 429.0. 3EG J1746-2851 sits in the most densely-packed region of the high-energy gamma-ray sky; there are ten sources listed in the 3rd EGRET Catalog within  $10^\circ$  of the Galactic Center. Given the broad EGRET PSF, source confusion is a serious problem. However, while 3EG J1746-2861 appears to fluctuate during two different VP's, no other sources in confused regions display any evidence of short-term variability.

The light curve of 3EG J1746-2851 during VP 16.0 is shown in Figure 2. The three strongest one-day detections fall on days 7-9 of the two-week VP, during which the aspect was  $20^\circ$ . The peak detection has a significance of  $4.3\sigma$  and is flanked by detections of  $3.9\sigma$  and  $3.1\sigma$ . The variability index is 2.09, corresponding to a probability of 0.008 that these data are consistent with a nonvariable source. Monte Carlo analysis is more restrictive. This source and the seven others within a  $7^\circ$  radius were modeled and there is a probability of 0.0004 that a three-day fluctuation of this or greater significance will occur in a 14-day period given intrinsically nonvariable sources.

3EG J1746-2851 also shows evidence of variability in VP 429.0. During this pointing the aspect is only  $6^\circ$  and  $V = 3.0$ . The peak flux is  $(6.4 \pm 1.7) \times 10^{-6}$  photons  $\text{cm}^{-2} \text{s}^{-1}$  and on two days the source is not detected at all, but there is no evidence of flaring.

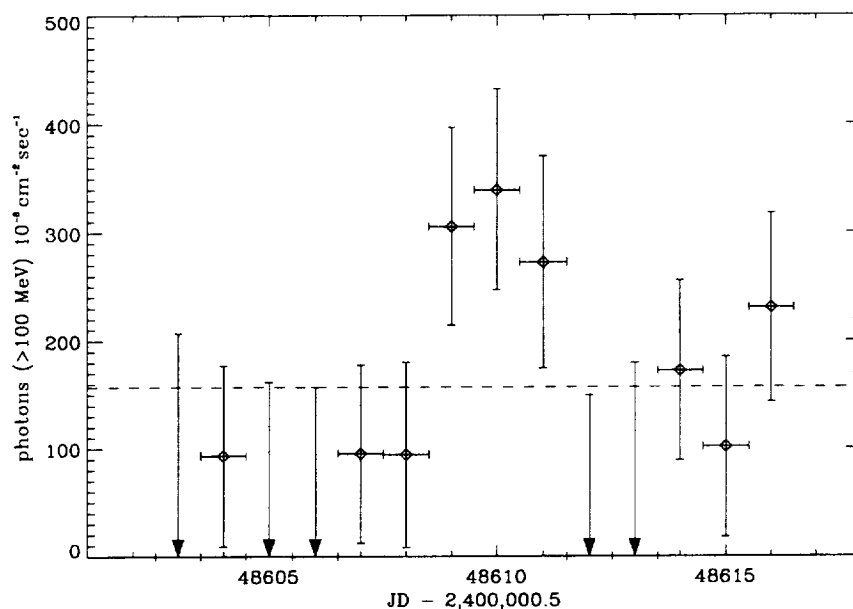
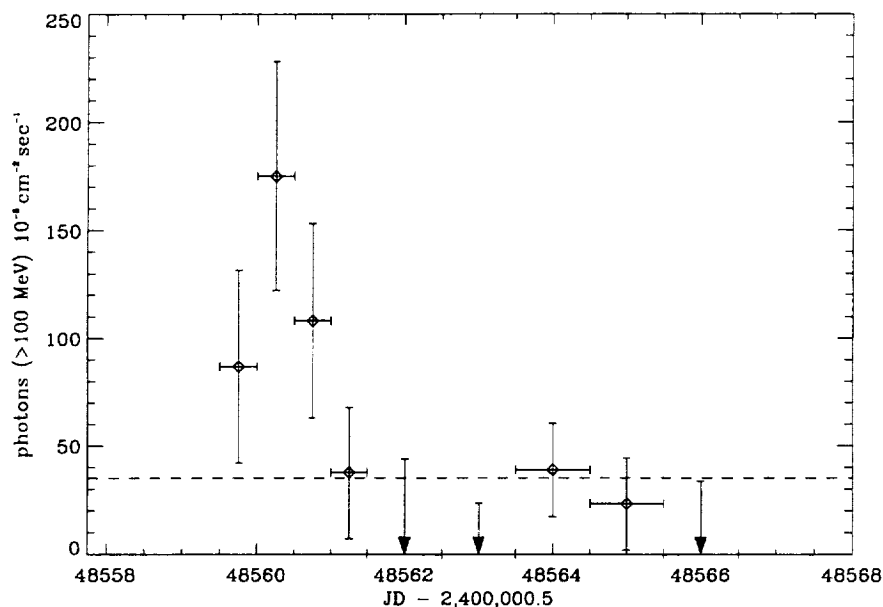


FIGURE 2. Light curve of 3EG J1746-2851 from VP 16.0.  $V = 2.09$ .

## 3EG J2006-2321

This source shows strong variability in VP 13.1, during which it was  $13^\circ$  from the instrument axis. The light curve shows evidence of flaring and is shown in Figure 3. The variability index for this curve is 3.18; the Monte Carlo probability that the source is nonvariable is 0.0006. 3EG J2006-2321 is well-isolated and lies  $26^\circ$  off the Galactic Plane, free of the bright galactic diffuse radiation; thus the claim of variability is strengthened.

The combination of large  $|b|$  and flaring behavior suggests an association with the blazar class of AGN. However, all of the 66 3EG sources identified as AGN are associated with loud spectrally flat radio sources; for 3EG 2006-2321 no such association can be easily made. The best candidate is the radio source PMN J2005-2310 (260 mJy at 4.85 GHz,  $\alpha_r$  not known), for which the probability of association<sup>4</sup> with 3EG J2006-2321 is only 0.015. If this source is of extragalactic origin, then it is unlike other EGRET AGN; of the 10 AGN with peak flux above  $10^{-6}$  photons  $\text{cm}^{-2} \text{s}^{-1}$ , none are weaker than 1.0 Jy at 4.85 GHz.



**FIGURE 3.** Light curve of 3EG J2006-2321 from VP 13.1.  $V = 3.18$ . The first 4 points represent 12-hour integration times; the final 5 represent 24-hour integration times.

Recently, two other sources have been found to share this combination of variability, peak flux above  $10^{-6}$  photons  $\text{cm}^{-2} \text{s}^{-1}$ , and lack of easy association with a radio-loud spectrally flat counterpart: 2CG 135+01 and GRO J1838-04<sup>5,6</sup>. An association of 2CG 135+01 (3EG J0241+6103) with the radio source GT 0236+610 has been suggested but not confirmed; GT 0236+610 itself is associated with the massive binary system LS I +61°303. To date there are not plausible counterparts, galactic or extragalactic, for GRO J1838-04 (3EG J1837-0423). 3EG J2006-2321,

along with these two sources, may be representative of a new class of high-energy gamma-ray emitters. However, there are some differences among these three sources; unlike 3EG J2006-2321, the other two sources are very close to the Galactic Plane. Also, while 2CG 135+01 is found by the present study to be variable on short time scales, GRO 1838-04 is not; it is a very bright but steady source in VP 423.0.

Further study of possible association of this source with PMN J2005-2310 is underway.

## CONCLUSION

The survey of EGRET data from cycles 1-4 finds three unidentified sources that display some evidence of short-term variability; large statistical errors ensure that we detect only the strongest variations. Of these three, only 3EG J2006-2321 is strongly variable. If this source is an AGN, its radio characteristics are unlike those of other bright (peak flux  $> 10^{-6}$  photons  $\text{cm}^{-2} \text{s}^{-1}$ ) EGRET blazars. If it is not extragalactic in origin, it may, with 2CG 135+01 and GRO J1838-04, represent a new class of high-energy gamma-ray emitters. Study of this source continues.

## REFERENCES

1. Hartman, R. C. et al. 1999 ApJS, 123, 79
2. Sturmer, S. J. & Dermer, C. D. 1995, A&A, 293, L17
3. Mayer-Hasselwander, H. A. et al. 1998, A&A 335,161
4. Mattox, J. R. 1999, these proceedings
5. Kniffen, D. A. et al. 1997, ApJ, 486, 126
6. Tavani, M. et al. 1998, ApJ, 497, L89

